Design and Study of Novel Fluorinated Tags for Elucidation of Protein Conformational Dynamics by ^{19}F NMR

by

Jerome Gould

A thesis submitted in conformity with the requirements
for the degree of Master of Science

Chemical & Physical Science
University of Toronto

Design and Study of Novel Fluorinated Tags for Elucidation of Protein Conformational Dynamics by ^{19}F NMR

Jerome Gould

Master of Science

Chemical & Physical Science
University of Toronto

2019

Abstract

Here we explore a variety of monofluorinated and trifluoromethyl reporters in an effort to derive optimal tags for purposes of fluorine NMR studies of proteins. By examining fluorine NMR spectra in MeOH and water mixtures, we compared chemical shift sensitivity to solvent polarity. A bromo-acetamide functionalized monofluorinated pyridinol, which was designed to be specifically reactive towards thiols, was observed to exhibit an unprecedented range of chemical shift dispersions of 2.56 ppm in these solvents. A trifluoromethylated analog exhibited a chemical shift range of 1.67 ppm albeit with higher intensity and reduced linewidth. This may be contrasted with conventional fluorinated tags such as BTFA and BTFMA, whose dispersions are on the order of 0.57 and 1.03 ppm, respectively. We anticipate that these next-generation tags will greatly enhance prospects for fluorine NMR studies of proteins and fluorine NMR based drug discovery.

Acknowledgments

« I would like to thank Dr. R. Scott Prosser for giving me the opportunity to conduct research in his laboratory, as well as, his guidance in this project; to Advait Hasabnis for his support and insight; Alexander Orazietti for showing me the basics of protein expression and providing me with a calmodulin mutant that I could use for testing my fluorinated tags; Shuya (Kate) Huang for using my tags to label her g-protein and for providing me the NMR spectra from them; to Dr, Peter M. MacDonald for offering his knowledge and support; to everyone else in the Prosser lab for their support, and Leizl Polinario for her contribution towards the project.»

Table of Contents

List of Tables

List of Figures

List of Appendices

Chapter 1

Introduction

1.1 NMR

1 Nuclear magnetic resonance (NMR) spectroscopy is a key spectroscopic method used to understand structure and dynamics of both small and large molecules. Signal can be discerned from the majority of isotopes found on the periodic table. Common solution state NMR applications typically take advantage of NMR signals from ^{1}H, ^{13}C, ^{15}N, ^{31}P and ^{19}F. In NMR, the frequency of the resulting signal is based on the induced electromagnetic field from the magnetic moment associated with the nuclear spins, when placed in a magnetic field, and can be expressed using the following equation:[1]

$$B_{eff} = B_0 - \sigma B_0 \qquad (1.1)$$

Where B_{eff} is the effective field strength felt by the nucleus of an atom that has a magnetic moment which differs from the imposed field (B_0), and σ is a dimensionless shielding constant. The shielding constant is comprised of three terms (eq 1.2):

$$\sigma = \sigma_{dia} + \sigma_{para} + \sigma^{i} \qquad (1.2)$$

The diamagnetic term, σ_{dia}, corresponds to the opposing field resulting from the effect of the imposed field upon the electron cloud surrounding the nucleus. Thus, electrons closer to the nucleus result in greater shielding (i.e. s-orbital electrons) than distant ones (i.e. p-orbital electrons). The paramagnetic term, σ_{para}, comes from the excitation p electrons by the external field, and its impact is opposite to that of the diamagnetic shielding. Finally, the term, σ^{i}, is derived from the effects of neighboring groups, which may increase or decrease the field of the nucleus. The shielding constant can also be influenced by intermolecular effects; in most cases it arises from interactions with the solvent.[2]

The fluorine nucleus, ^{19}F, has an abundance of 100%, and contains one of the highest gyromagnetic ratios, next to tritium and ^{1}H nuclei, providing excellent sensitivity for NMR, as well as, short relaxation times.[3] While possessing an identical spin ½ nucleus to ^{1}H, ^{19}F it has a much greater chemical shift range and sensitivity to the local environment (electronic environment, solvent polarity, and concentration).[4] The large chemical shifts observed in ^{19}F are attributed to the 9 electrons surrounding the nucleus, specifically the p electrons which are easily polarizable, resulting in range of ~1100 ppm, whereas ^{1}H has a chemical shift range of ~20 ppm.[2,3]

Depending on the placement of fluorine on a molecule, fluorine's electron withdrawing properties can be used to alter the pKa of proximal atoms due to charge stabilization, thus increasing or decreasing the probability of protonation. The strong electronegativity of the fluorine substituents can also lower the pKa for alcohols and carboxylic acids, and increase the pKa for amines. Fluorine substituents can also be used to enhance bioavailability and lipophilicity which is important for biologically active compounds, since it often controls absorption, transport, or receptor binding.[5,6]

In terms of studying macromolecules using NMR spectroscopy, proteins demonstrate a relationship between structure and function, in which the conformation of the protein is in an active, inactive, or intermediate state. If the structure of a protein present in a chemical signaling pathway can be deduced, certain conditions can be applied to manipulate and shift the protein towards a certain conformational state, typically through the application of various drugs.[7]

1.2 Use of ^{19}F NMR in Protein Studies

In ^{19}F NMR protein studies, fluorine can be introduced into the protein by substituting an amino acid with a fluorinated amino acid derivative. This is typically achieved through incorporation of the fluorinated amino acids into the biosynthesis process of the protein in a living organism, usually bacteria or yeast. The changes in chemical shifts in this case would be caused by local secondary and tertiary structures, solvent exposure, and conformational dynamics rather than variations in chemical structure.[3] Tryptophan residues in a protein, for example, can be replaced with a fluorinated tryptophan analog, producing distinct signals for each position containing a tryptophan in the given sequence.[8] Formation of a complex between a fluorinated small molecule and a receptor will also experience a change in its chemical shift, due changes in the

local environment.[9] The sensitivity to environmental changes is ideal in many protein studies for purposes of delineating distinct conformers or states, and through relaxation experiments, the interconversion rates and lifetimes.[10]

^{19}F NMR has shown significant results in with respects to elucidating protein folding and unfolding, as well as, various protein interactions and activity.[11] In G-protein coupled receptors (GPCRs), a wide range of signaling behaviors can be observed. A fluorinated thiol specific tag 3-bromo-1,1,1-trifluoroacetone (BTFA) was used to label a specific cysteine residue on the β2 adregenic receptor (β2AR), revealing multiple conformational states based on solvent exposure of the cysteine residue upon the application of ligands.[10]

^{19}F NMR serves to delineate structures primarily in complex biological molecules that may be cumbersome for traditional HCN NMR techniques.[11] By incorporating fluorine into proteins through biosynthetic or post-translational means, 1D ^{19}F experiments can be conducted for characterization of local environmental changes through its relative chemical shift dispersion. The fluorine signal will also be prominent due to absence of natural fluorine in most biological systems, thus it is can be extremely useful for *in vivo* drug studies.[12]

1.3 Need for Higher Resolution Tag

The chemical shift for fluorine is known to be strongly influenced by long-ranged electrostatic effects[13], such as, van der Waals interactions, local magnetic effects from aromatic ring currents electronically anisotropic species, and solvent accessibility which contribute to differences in the shielding of the fluorine nucleus. The electrostatic effects and van der Waals interactions are also able to couple with the lone pair electrons on fluorine leading to a significant change in the paramagnetic shielding term.[14] For example, placing an electron withdrawing group, such as a carbonyl, adjacent to trifluoromethyl group will generally result in strong shielding effects being exerted on the fluorine nuclei.[4]

Other moieties can also contribute to the effective partial charge experienced by the CF_3 group, resulting in changes in the shielding of the fluorine nuclei. The polarizability, and molecular geometry of the species adjacent to the CF_3 group can also impact the range of shielding effects, and thus the sensitivity of fluorine to its local environment. Steric hinderance around the CF3 can

physically shield it from solvents or the local environment, thus reducing the overall sensitivity to the environment.[3,15,16]

In many of these ^{19}F NMR studies of proteins, the chemical shift of the probe is dependent on local environmental changes caused by secondary and tertiary structures. The differences in solvent exposure may be subtle, resulting in poor resolving capability for the spectra. As a result, investigation for chemical probes with greater sensitivity to local environmental changes is required in order to obtain greater resolving capability.

Investigation for a more effective probe has been previously explored. A survey of various thiol-specific fluorinated tags was conducted by Ye *et al.* (2015), showing that 2-bromo-N-(4(trifluoromethyl)phenyl)acetamide (BTFMA) had a greater response to changes in solvent polarity in comparison to other common probes, such as, 2,2,2-trifluoroethyl-1-thiol (TFET) and BTFA. This was attributed to the presence of an aromatic ring conjugated to a trifluoromethyl group which proved to greatly enhance sensitivity to electrostatic interactions through ring current effects.[3]

Using the same methodology as Ye et al. (2015), we make use of solvent mixtures which provide a wide range of dielectric environments to explore chemical shift sensitivity of new ^{19}F NMR tags to environment.[3] In a protein, we would expect to observe a similar range of solvent accessibility and electrostatics from micro-environments. Thus, the chemical shift sensitivity to dielectric environment provides a simple way to predict chemical shift sensitivity of a tag in a protein NMR study. Here, we make use of varying ratios of water to methanol and we explore various small molecules in hopes of finding a species that is more sensitive to local environment then BTFMA, thus allowing for greater spectral resolvability. This project primarily focuses on tautomeric species as potential candidates, since their electronic structure and their tautomeric equilibria are both very sensitive to dielectric environment. Thus, we anticipate an amplification in the range of observable chemical shifts for certain tautomers, depending on the placement of the ^{19}F or CF_3 tag with respect to the tautomer.[17]

Chapter 2

Experimental Method

2.1 Sample Preparation

2 Chemicals were obtained commercially. Preparation of 10.0 mM stock solutions were prepared by dissolving the compound in 1 mL MilliQ water (or methanol if they were not soluble in water).

2.1.1 External Reference

An external reference was utilized to avoid changes in chemical shift of the compound of interest, in addition to, isotopic effects from deuterated solvent, as well as, keeping the reference constant between samples. Using an external reference also allowed for easier acquisition of 1D ^{19}F NMRs at higher percentages of methanol. NaF, and TFA were used as external references. For NaF, a 20.0 mM solution was made using 0.84 mg of NaF dissolved in 1 mL D_2O. For TFA, a 2.5 mM solution was made using 192.6 µL dissolved in 1 mL D_2O. Pasteur pipettes with a long capillary tip were flamed shut over a Bunsen burner and cooled at room temperature before dispensing the reference solution into it. The Pasteur pipette was then flamed at a height slightly above that of an NMR tube, thus sealing it at both ends. A hole was created on an NMR cap, and the external reference was passed through allowing it to be placed roughly center in the NMR tube. TFA appears at -62.48 ppm, and NaF appears at -122.44 ppm.

2.1.2 Buffer Solutions

Buffer solutions for 50mM pH 5.0 and 0.2 M pH 5.5 were made using NaOAc and HOAc. For 0.2 M pH 6.0, 0.1 M pH 6.5, 0.1 M pH 7.0, and 1.0 M pH 7.4, Na_2HPO_4 and NaH_2PO_4 was used. For 50 mM pH 8.0, 50 mM pH 8.5, and 50 mM pH 9.0, Trizma HCl and Trizma base was used. Buffer solutions were adjusted using an Orion pH Meter 420 with 0.1 M NaOH and 0.1 M HCl.

2.1.3 Polarity Series

A polarity series was created using 50 µL of the 10.0 mM stock solution of the compound of interest and diluted with an increasing ratio of methanol to MilliQ water. Table 1 summarizes the volumes used for the polarity series with a final sample concentration of 0.5 mM. When using a buffered solution, the final buffer concentration was adjusted to 50 mM in MilliQ water.

Table 2-1 Summary of volumes used to obtain varying polarity index's using water and methanol, with a final sample concentration of 0.5 mM.

MeOH (%)	Sample (µL)	MeOH (µL)	MilliQ Water (µL)**	Polarity Index
0	50	0	950	10.2
5*	50	0	950	9.945
25	50	250	700	8.925
50	50	500	450	7.65
75	50	750	200	6.375
95	50	950	0	5.355
100*	50	950	0	5.1

*10.0 mM stock solution of sample is made in MeOH.
**Amounts are equivalent for 50 mM buffer solutions.

2.1.4 Conjugation of GSH to Thiol Reactive Tags

Glutathione (GSH) conjugation was done for thiol reactive tags. GSH and the tag were mix in 5:1 ratio to insure formation of product, with final concentrations of 5 and 1 mM in 1 mL MilliQ water. Solutions which were analyzed via ESI-LC/MS were done without buffer so that samples can easily be run through the ESI-LC/MS. Solutions were vortexed and left at room temperature for approximately 24 hours, then run through the ESI-LC/MS. Additionally samples that were analyzed using NMR were buffered to the desired pH and examined for 24 hours to track the progress of the reaction.

2.2 Data Collection & Analysis

2.2.1 ESI-LC/MS

ESI-LC/MS was used to confirm and monitor the conjugation reaction by running solutions with and without GSH. All samples that were run on the LC/MS did not contain any buffer to bypass having to desalt the solutions. Solutions containing GSH were given 0.1% TFA and vortexed prior to running to ensure samples were positively charged. ESI-LC/MS was also used to check and confirm products from synthetic reactions. Products from synthetic reactions were not treated with 0.1% TFA and were instead run in both positive and negative ESI. The flow rate

was set to 50 µL/min, and the spectra were acquired with 30 scans with a range of M/Z between 100 and 700.

2.2.2 Acquisition of 1D ^{19}F Spectra

19F NMR spectra were obtained using a 600 MHz Varian spectrometer, equipped with a quadres probe tuned to 19F. The following pulse sequence is an example of what was used for the 1D ^{19}F NMR spectras:

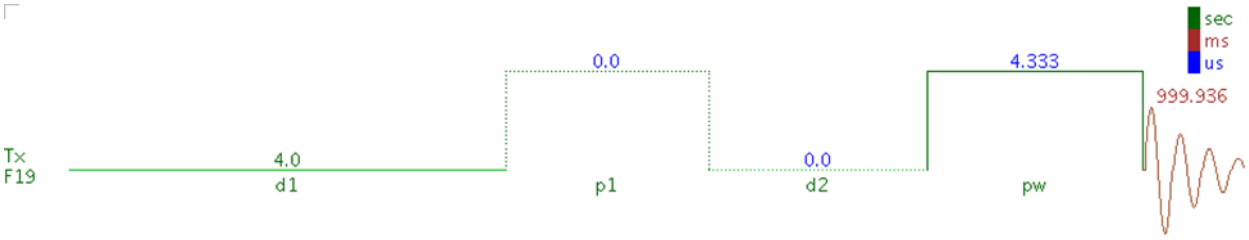

Figure 2-1 Pulse sequence used for 1D ^{19}F experiments.

128 scans were acquired for each spectra and were processed using MesReNova 11.0 software. A 400 MHz Brucker spectrometer was primarily used for ^{1}H and ^{13}C NMR experiments.

2.3 Functionalization of Tags

Functionalization of 6-TFHP and 5-MFHP was done using commercially available alkyl bromide functionalized compounds. 37% methylamine was used in excess and was stirred for 3 hours before drying using rotary evaporation. The compound was furthered dried overnight using a desiccator. The compound was dissolved in DMF and 1.5 equivalence of bromoacetyl bromide was added and stirred for around 8 hours, then dried using rotary evaporation. Purification was conducted using a silica column and 5% MeOH in DCM (Figure 3-11).

Chapter 3

Results & Discussion

3.1 Tautomerism

3 Model studies and density functional theory (DFT) studies have been performed for β_2AR tagged with BTFMA. These studies suggested greater chemical shift sensitivity via the conjugation of a trifluoromethyl group onto an aromatic compound.[3] To further optimize sensitivity to changes in the local environment, the use of a tautomeric moiety was investigated due to their sensitivity to local environmental changes.

Tautomers are often prototrophic, leading to interconversions through a relocation of a proton:[18]

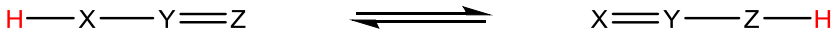

Some of the common tautomeric pairs are keto-enols, amide-imidic acid, amine-imine, and lactam-lactims which are a cyclic variant of amide-imidic acid (Figure 3-1).[19]

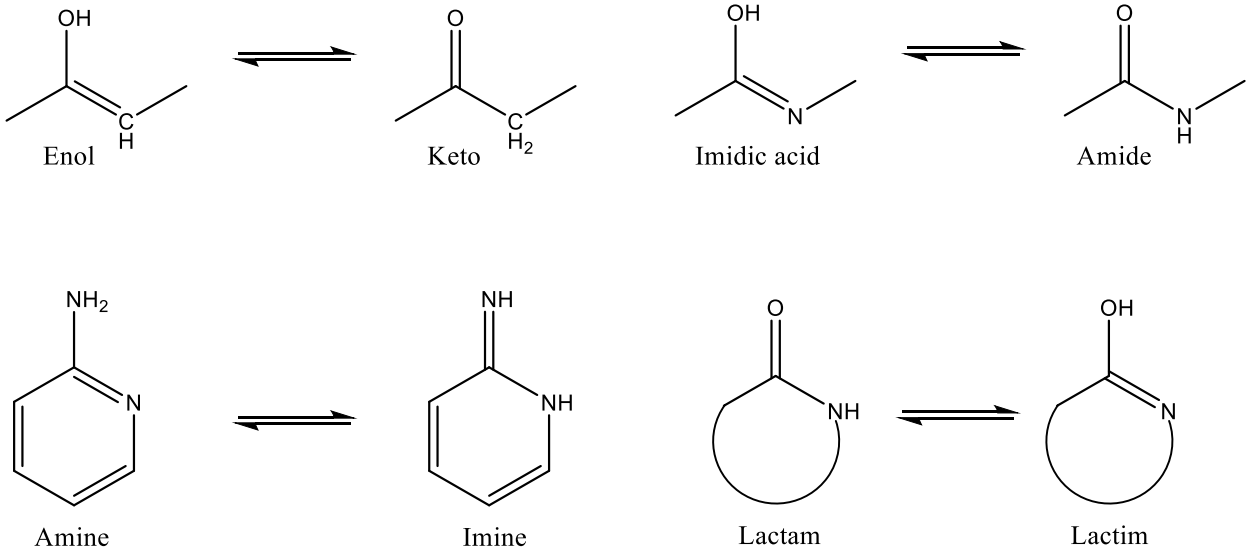

Figure 3-1 Example of common tautomeric pairs.

This project will focus on the tautomeric species known as beta-diketones, and pyridinols as potential candidates for amplifying the sensitivity to local environmental changes. In choosing the compounds for this investigation, commercially available compounds were prioritized, and size of compound were taken into consideration as perturbations caused from conjugation of the tag to a protein would ideally have minimal effects on the system, thus preventing or limiting unwanted secondary or tertiary structures.[3]

3.1.1 Beta-diketones

Beta-diketones are interesting as they possess up to three unique tautomeric states (Figure 3-2). When placing a trifluoromethyl group adjacent to the beta-diketone it is often observed that tautomerization from the diketo to the keto-enol state leads to a shift of the ^{19}F NMR resonance for the CF_3 group to a lower field, due to decreased shielding by the C=C enolic topology. Greater deshielding effects on the CF_3 group have also been observed when placing the beta-diketone in a smaller ring size, and with exocyclic keto-enol moieties. The diketo and keto-enol forms exist in slow exchange on an NMR timescale, manifesting as distinct peaks corresponding to each state. The chemical shift difference between the diketo and the keto-enol forms can vary up to 10 ppm, demonstrating a potential moiety that can further amplify the sensitivity of an adjacent CF_3 group to local environmental changes.[4]

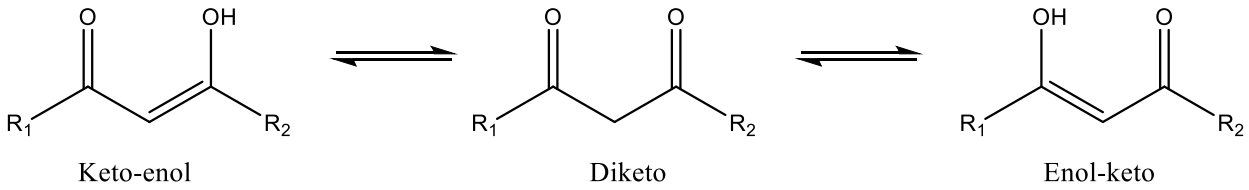

Figure 3-2 Beta-diketone tautomerism.

The beta-diketones chosen for this experiment are ethyl-4,4,4-trifluoroacetoacetate, which is among the simplest beta-diketones selected. 4,4,4-trifluoro-1-phenyl-1,3-butanedione, explores the effects of adding an adjacent aromatic ring as an electron withdrawing group (EWG), which had previous proven to increase sensitivity of BTFMA, and finally, 4,4,4-trifluoro-1-(bromophenyl)-1,3-butanedione, with the bromo group on ortho, meta, and para positions to examine the inductive effects of the bromine on the beta-diketone (Figure 3-3).

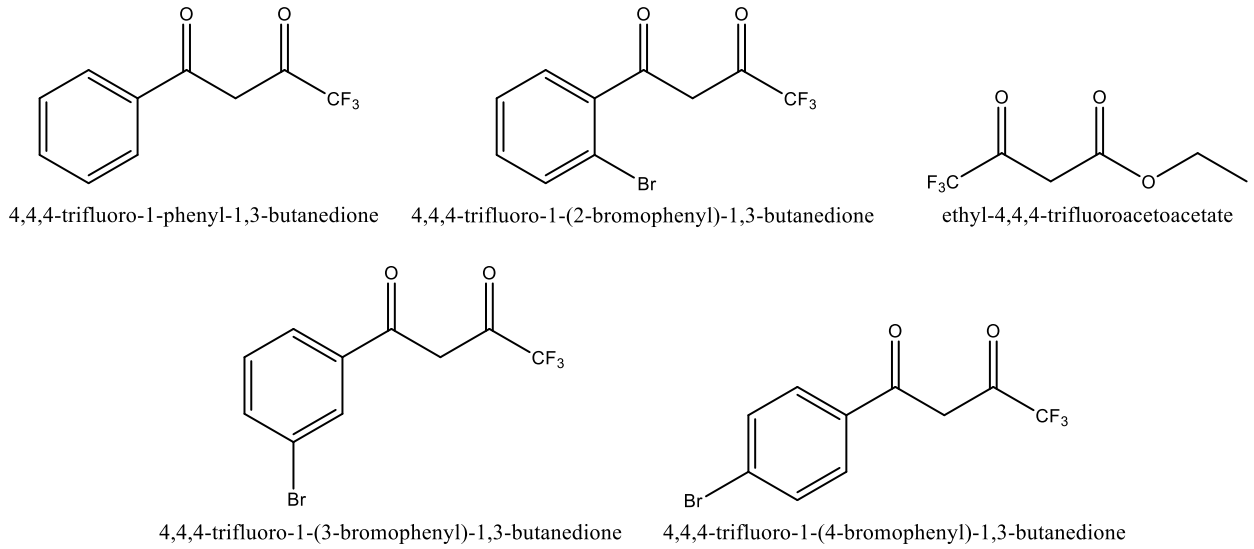

Figure 3-3 Structures of the beta-diketone compounds investigated.

3.1.1.1 Effects of Solvent Polarity

The effects of solvent polarity were explored using varying ratios of water to methanol, and the two to three peaks corresponding to each state were compared against one another. The peak(s) that manifest further downfield, around -75 ppm correspond to the keto-enol form, while the peak that further upfield, around -85 ppm corresponds to the diketo form.

For ethyl 4,4,4-trifluoroacetoacetate, two peaks were observed for the majority of the polarity series, where one peak was generally seen for the keto-enol. The first peak shows an overall shift of 1.16 ppm, while the second peak was 0.31 ppm and was only observed between 25-50% MeOH. The third peak corresponding to the diketo, had a chemical shift change of 0.97 ppm (Table 3-1).

Table 3-1 Summary of chemical shifts observed for ethyl 4,4,4-trifluoroacetoacetate at 25ºC with respect to solvent polarity.

Polarity Index	$\Delta\delta_1$ (ppm)	$\Delta\delta_2$ (ppm)	$\Delta\delta_3$ (ppm)	$\Delta\delta_{1\text{-}2}$ (ppm)	Peak Ratio of 1 & 2
10.2	0	-	0	-	-
8.925	0.07	0	0.05	0.04	0.554
7.65	0.39	0.31	0.36	0.03	12.434
6.375	0.74	-	0.72	-	-
5.355	1.16	-	0.97	-	-

For 4,4,4-trifluoro-1-phenyl-1,3-butanedione three peaks were observed. The first two peaks were representative of the keto-enol, while the third represents the diketo form. As solvent polarity decreased, the first peak showed a small shift of 0.42 ppm, while the second peak had a larger shift of 0.83 ppm and the third had a shift of 0.71 ppm. The ratio of the two peaks also shifted towards the second peak (Table 3-2). Compared to ethyl 4,4,4-trifluoroacetoacetate, the addition of the aromatic phenyl ring, seems to have decreased overall sensitivity of the beta-diketone, but increased sensitivity for the second peak corresponding to the keto-enol, as well as, the peak separation between the two keto-enol states.

Table 3-2 Summary of chemical shifts observed for 4,4,4-trifluoro-1-phenyl-1,3-butanedione at 25ºC with respect to solvent polarity.

Polarity Index	$\Delta\delta_1$ (ppm)	$\Delta\delta_2$ (ppm)	$\Delta\delta_3$ (ppm)	$\Delta\delta_{1\text{-}2}$ (ppm)	Peak Ratio of 1 & 2
10.2	0	0	0	0.04	3.375
8.925	0	0.02	0.15	0.02	0.109
7.65	0.2	0.37	0	0.21	0.094
6.375	0.36	0.55	0.35	0.23	0.076
5.355	0.42	0.83	0.71	0.45	0.017

For 4,4,4-trifluoro-1-(2-bromophenyl)-1,3-butanedione only two peaks were observed, where the diketo form was not present. The first peak shows an overall shift of 0.76 ppm, while the second peak is 0.91 ppm. The shift difference between the two peaks increases slightly with decreasing solvent polarity and the peak ratio shifts slightly towards peak 1, however, peak two remains dominant (Table 3-3). By adding a bromo group to the phenyl ring on the ortho position, we have biased the beta-diketone and increased overall sensitivity for the keto-enol form.

Table 3-3 . Summary of chemical shifts observed for 4,4,4-trifluoro-1-(2-bromophenyl)-1,3-butanedione at 25ºC with respect to solvent polarity.

Polarity Index	$\Delta\delta_1$ (ppm)	$\Delta\delta_2$ (ppm)	$\Delta\delta_3$ (ppm)	$\Delta\delta_{1\text{-}2}$ (ppm)	Peak Ratio of 1 & 2
10.2	0	0	-	0.48	0.111
8.925	0.08	0.10	-	0.50	0.103
7.65	0.28	0.35	-	0.55	0.123
6.375	0.58	0.70	-	0.60	0.128
5.355	0.76	0.91	-	0.63	0.143

For 4,4,4-trifluoro-1-(3-bromophenyl)-1,3-butanedione two peaks were observed for the majority of the polarity series, where the diketo form was not present. The first peak shows an overall shift of 0.38 ppm, while the second peak is 0.74 ppm. The shift difference between the two peaks increases with decreasing solvent polarity and the peak ratio shifts slightly more towards peak 2 (Table 3-4). Switching the bromo group to the meta position results in overall decrease in sensitivity with respects to both the phenyl group, and phenyl with the bromo group in the ortho position.

Table 3-4 Summary of chemical shifts observed for 4,4,4-trifluoro-1-(3-bromophenyl)-1,3-butanedione at 25ºC with respect to solvent polarity.

Polarity Index	$\Delta\delta_1$ (ppm)	$\Delta\delta_2$ (ppm)	$\Delta\delta_3$ (ppm)	$\Delta\delta_{1\text{-}2}$ (ppm)	Peak Ratio of 1 & 2
10.2	0	0	0	0.07	0.435
8.925	0.04	0.02	-	0.13	0.280
7.65	0.14	0.43	-	0.36	0.164
6.375	0.32	0.62	-	0.37	0.149
5.355	0.38	0.74	-	0.43	0.063

For 4,4,4-trifluoro-1-(4-bromophenyl)-1,3-butanedione only the polarity series was conducted, showing three peaks with the highest chemical shifts among the beta di-ketones. The first peak shows an overall shift of 0.73 ppm, while the second peak is 1.41 ppm, and the third peak is 1.07 ppm. The shift difference between the two peaks increases moderately with decreasing solvent polarity and the peak ratio shifts towards peak 2, however, peak two remains dominant (Table 3-5). When the bromo group is placed para to the beta-diketone, we experience the greatest effect with an increase sensitivity for all beta-diketone states.

Table 3-5 Summary of chemical shifts observed for 4,4,4-trifluoro-1-(4-bromophenyl)-1,3-butanedione at 25ºC with respect to solvent polarity of the solution.

Polarity Index	$\Delta\delta_1$ (ppm)	$\Delta\delta_2$ (ppm)	$\Delta\delta_3$ (ppm)	$\Delta\delta_{1\text{-}2}$ (ppm)	Peak Ratio of 1 & 2
10.2	0	0	0	0.40	7.015
9.945	0.02	0.13	0.01	0.25	11.894
8.925	0.10	0.12	0.04	0.42	8.452
7.65	0.33	0.67	0.17	0.74	4.420
6.375	0.60	1.17	0.56	0.97	2.446
5.1	0.73	1.44	1.07	1.11	0.789

Although some of these compounds demonstrate chemical shifts greater or equal to BTFMA, they are generally more complex to analyze due the multiple states present. The peak intensities can also vary, making it non-ideal for use as a ^{19}F chemical probe for protein labeling. However, it may be able to convey more information than what can be ascertained from a single peak but would require extensive modeling to be of any use. Another drawback is that the intensity can effectively be reduced by 1/2 to 1/3 depending on how many states are present at a given moment, since the beta-diketone can only exist in one state at any given time. While the beta-diketones did show some promising chemical shift changes with respects to solvent polarity, they ultimately not ideal for protein labeling with respects to solvation effects.

3.1.1.2 Effects of pH

The beta-diketones, while they were not ideal from the perspective of solvation effects, they demonstrate significant changes in state populations with respects to pH. For the beta-diketones the pH was varied between pH 5,7, and 9 to see how they behave under acidic, neutral, and basic conditions, respectively. The general trends that were observed for the beta-diketones were that the diketo form was predominant under acidic conditions, and as pH increased the states shifted more towards the keto-enol form. From neutral to basic pH we also observe that there is typically a shift in state populations in the two peaks corresponding to the keto-enol forms (Appendix 6-10).

3.1.2 Pyridone

Using aromatic heterocycles, such as, pyridone (or pyridinol) non-equivalent aromatic structures can be obtained through tautomerization, resulting in two constitutional isomers (Figure 3-4), which combines an environmentally dependent deshielding functional group and an aromatic system resulting in greater sensitivity to local environment.

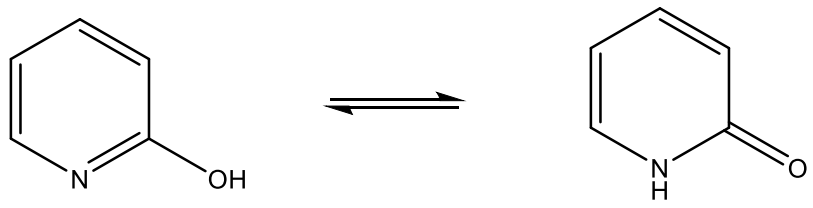

Figure 3-4 Pyridone tautomerism.

A series of pyridones were investigated with the CF_3 group at various positions to determine the optimal position. The mono-fluoro equivalent of the CF_3 group were examined as well, since it is predicted to be more susceptible to aromatic ring current effects. Other pyridinol variants were also explored to see how tautomerism amplifies chemical shift sensitivity (Figure 3-5).

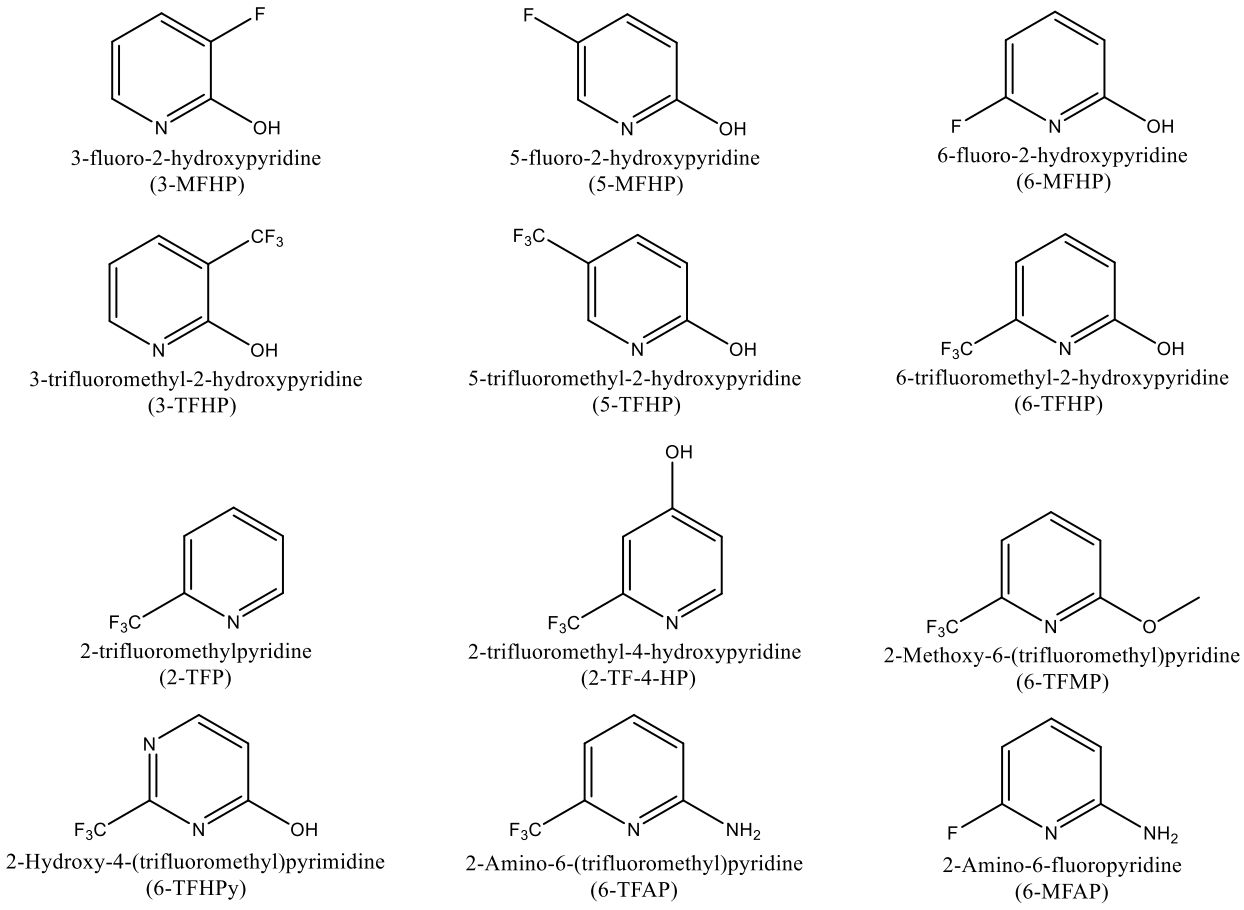

Figure 3-5 Structure of pyridone and related molecules.

3.1.2.1 Effects of Solvent Polarity

Similar to the beta-diketones, the pyridones were examined under various ratios of water to methanol. Unlike the beta-diketone, the tautomerism is in fast exchange for the pyridones, resulting in one peak that is the population-weighted average of the two tautomeric states. As a result, the spectras obtained are much simpler, and allow for a larger chemical shift range with respect to local environmental changes.

Using just an aromatic heterocycle, 2-trifluoromethylpyridine (2-TFP) a significantly higher chemical shift range ($\Delta\sigma_{polarity}$ = 1.23 ppm) was observed over that seen in BTFMA ($\Delta\sigma_{polarity}$ = 1.03 ppm) for an identical range of solvent polarity in MeOH/water mixtures. Looking at the pyridones, we observe that almost of them possess chemical shifts greater than BTFMA, with the exception of 5-trifluoromethyl-2-hydroxypyridine (5-TFHP), and 2-hydroxy-4-(trifluoromethyl)pyrimidine (6-TFHPy) which have chemical shift ranges of 0.91 ppm, and 0.96, respectively. In the case of 5-TFHP, this may be the result of the pi-electron density being pulled towards the lactim-lactam, causing a decrease in aromatic ring current effects on that region of the aromatic ring.[20] Conversely, 3-trifluoromethyl-2-hydroxypyridine and 6-trifluoromethyl-2-hydroxypyridine have chemical shifts ranges of 1.24 and 1.61 ppm, respectively, which may be attributed to the increased pi-electron density within the vicinity of the CF_3 group, where the effects from the nitrogen on the aromatic ring are greater than experience from the keto-enol.

2-trifluoromethyl-4-hydroxypyridine (2-TF-4-HP), 2-methoxy-6-(trifluoromethyl)pyridine (6-TFMP)), and 2-amino-6-(trifluoromethyl)pyridine (6-TFAP) were examined to see how much tautomerism amplifies or effects the sensitivity to the local environment. By methylating the hydroxyl group and preventing the pyridone from tautomerizing, 6-TFMP demonstrates a decrease in chemical shift range with a 1.52 ppm shift. Placing the hydroxyl group para to the nitrogen on the aromatic ring, still allows for tautomerism since it is a concerted mechanism, results in a chemical shift range of 1.49 ppm.[19] In 6-TFAP, replacing the hydroxyl with an amino group should still allow for tautomerism, but is not as electron withdrawing as the hydroxyl group, leading to reduced chemical shift range of 1.37 ppm (Figure 3-6).

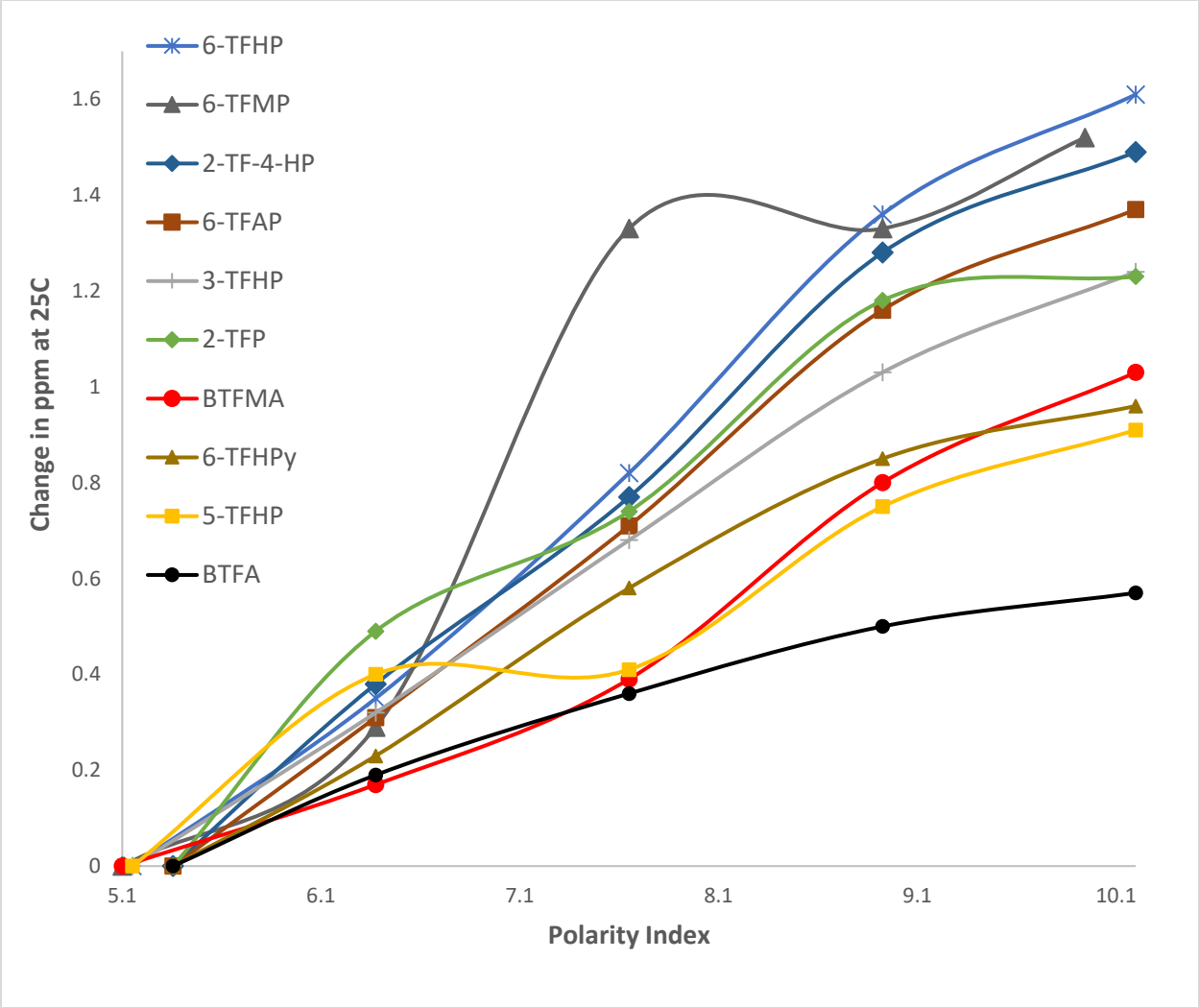

Figure 3-6 Summary of chemical shifts observed for various trifluoromethyl pyridone compounds at 25°C. Solutions were made in various ratios of MeOH to H_2O, where a polarity index of 5.1 represents 100% MeOH and 10.2 is 100% H_2O.

Looking at some monofluoro analogs, we observe extremes where the pyridone is either very sensitive or very insensitive to the local environment. 3-fluoro-2-hydroxypyridine (3-MFHP) demonstrates a chemical shift range of 0.03 ppm. 5-fluoro-2-hydroxypyridine (5-MFHP), and 6-fluoro-2-hydroxypyridine (6-MFHP) both demonstrate remarkable chemical shift ranges of 2.56 and 2.59 ppm, respectively. This was expected based on DFT calculations done by Ye *et al.* (2015) which determined that the effects from ring currents would be 2-3x greater when the fluorine is placed on the ring.[3] With 2-amino-6-fluoropyridine (6-MFAP) the chemical shift range dropped considerably showing a 0.15 ppm shift (Figure 3-7).

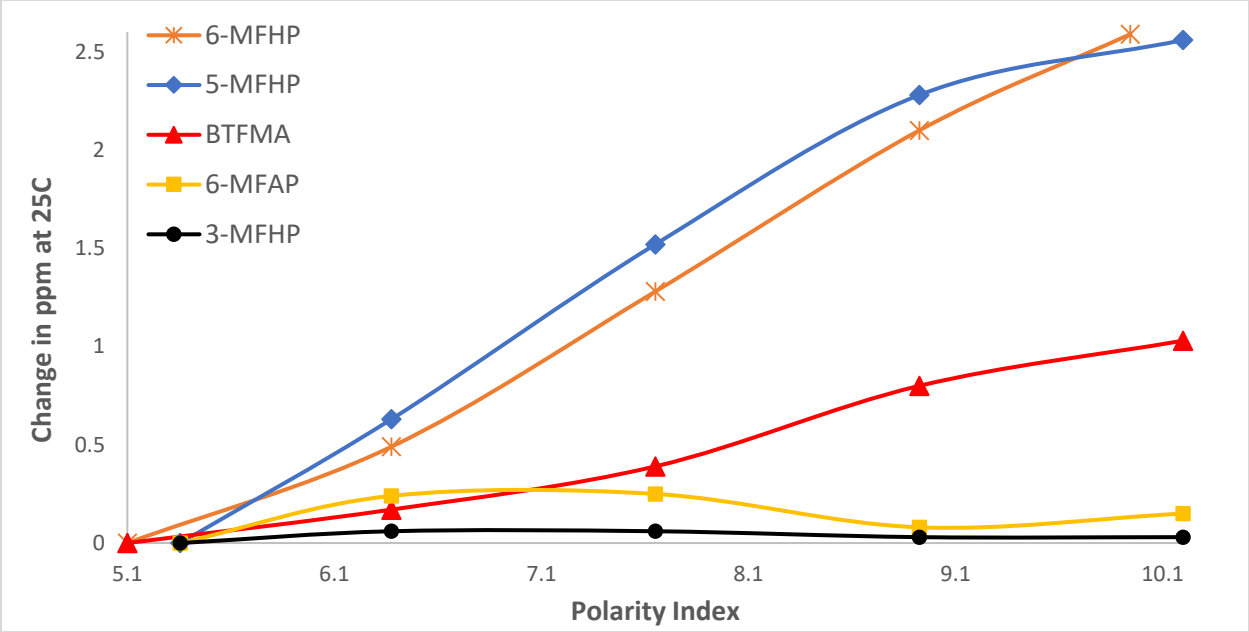

Figure 3-7 Summary of chemical shifts observed for various monofluoro pyridone compounds at 25°C. Solutions were made in various ratios of MeOH to H_2O, where a polarity index of 5.1 represents 100% MeOH and 10.2 is 100% H_2O.

3.1.2.2 Effects of pH

The effects of pH were briefly explored using 6-TFHP, since it was among the most sensitive CF_3 pyridones tested, to determine how it influences the lactim-lactam tautomerism. From pH 5 to 6 there is no change in chemical shift, and pH 6.5 to 9 gives a relatively linear response with an over chemical shift range of 0.58 ppm (Figure 3-8).

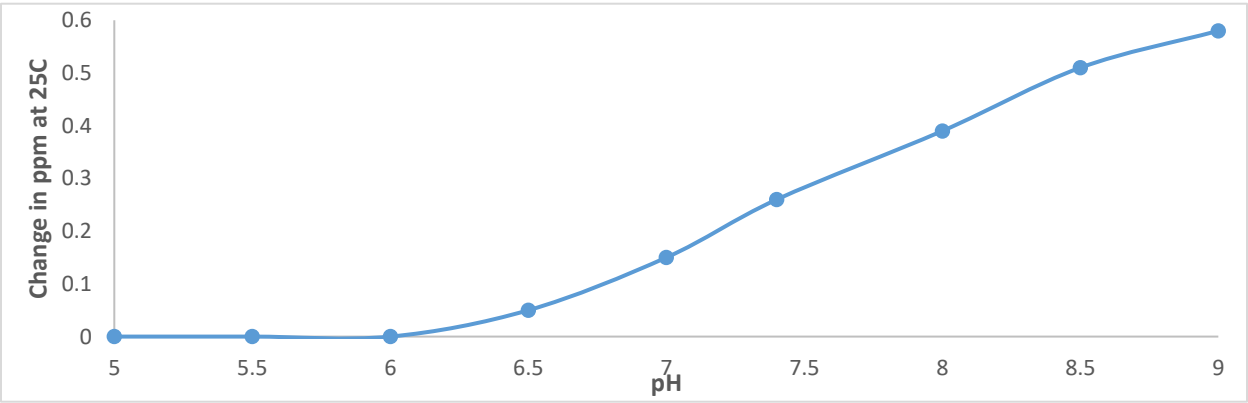

Figure 3-8 Change in chemical shifts observed for 6-TFHP under various pHs conditions at 25°C.

3.1.2.3 Effects of Temperature

To determine if the chemical shift range could be further increased the effects of temperature were explored for some of the CF_3 pyridones, since it can also influence the tautomeric equilibrium.[21] Relative to 15ºC the trifluoro species tend to become more sensitive to its local environment, where as the monofluoro species becomes less sensitive when temperature is increased (Table 3-6)Table 3-6 Summary of chemical shifts changes observed for various pyridone compounds at various temperatures..

Table 3-6 Summary of chemical shifts changes observed for various pyridone compounds at various temperatures.

^{19}F Tags	Range of MeOH to H_2O used (%)	$\Delta\delta$ (ppm) at 15ºC	$\Delta\delta$ (ppm) at 25ºC	$\Delta\delta$ (ppm) at 45ºC
BTFMA	0 – 100	0.95	1.03	1.22
5-MFHP	0 – 95	2.57	2.56	2.41
3-TFHP	0 – 99	1.16	1.24	1.39
5-TFHP	0 – 99	0.83	0.91	1.1
6-TFHP	0 – 99	1.59	1.61	1.65

3.2 Non-Tautomeric Species

Investigation into other non-tautomeric electron withdrawing species was conducted in order to other factors (e.g. electron-withdrawing/donating effects). 5-amino-2-nitrobenzotrifluoride, 3-fluoro-4-nitroaniline, and 1-fluoro-2,4-dinitrobenzene were chosen due to the strong meta directed NO_2 electron-withdrawing group (EWG). 1-(bromomethyl)-3-(difluoromethyl)benzene was examined as an analog to BTFMA with a CF_2H group instead of a CF3. 2-bromopropyl trifluoromethyl sulfone (BTFS) which possess a similar structure to BTFA was examined as the sulphone group should be strongly electron withdrawing. 3-bromo-1,1,1-trifluoro-propan-2-ol (BTFP) is also an analog to BTFA and demonstrated great potential, thus sparking further interest into variant structures that would not possess a chiral center. 2-trifluoromethyl-2-propanol serves as a baseline for a BTFP analog with an achiral center. 1,1,1,3,3,3-hexafluoro-2-methyl-2- propanol, and 1,1,1,3,3,3-hexafluoro-2-phenyl-2- propanol were considered to explore the effects of using two CF3 groups, as well as, the effect of using an adjacent EWG (Figure 3-9).

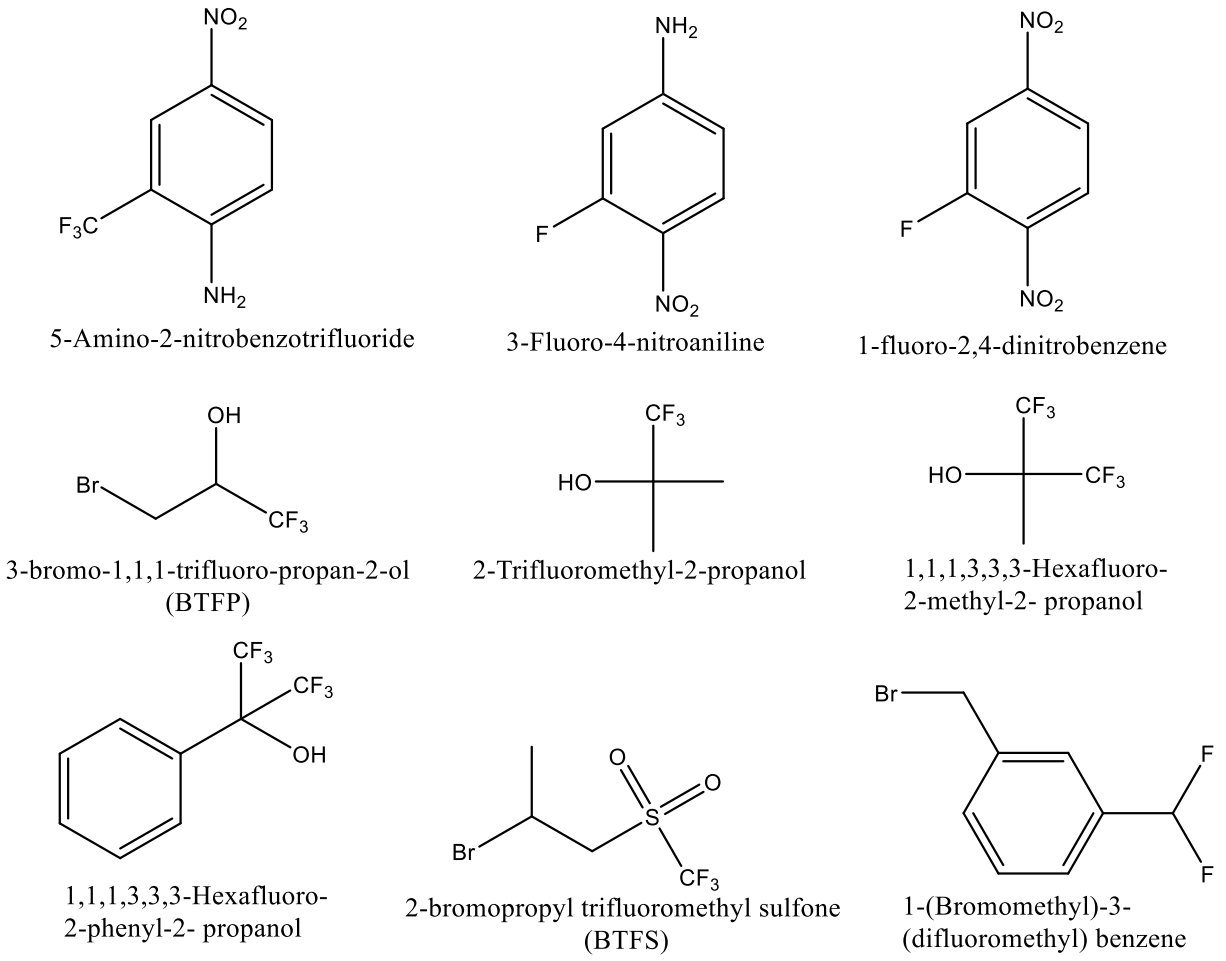

Figure 3-9 Structure of various other compounds investigated.

The effects of solvent polarity were explored for the numerous non-tautomeric compounds using varying ratios of water to methanol. 5-amino-2-nitrobenzotrifluoride had the lowest chemical shift range (0.81 ppm) among the non-tautomeric compounds and may be attributed to the adjacent amino group adding electron density into the ring. The monofluoro analog, 3-fluoro-4-nitroaniline had a chemical shift range of 1.49 ppm, although it has a greater chemical shift than its counterpart, it appears that the addition of an electron-donating group (EDG) onto the ring dampens the sensitivity of the fluoro group. 1-fluoro-2,4-dinitrobenzene showed the greatest chemical shift range of 1.99 ppm, signifying that more EWGs on the aromatic ring may prove to be advantageous in enhancing the sensitivity of the CF_3 group. 1-(bromomethyl)-3-(difluoromethyl)benzene a difluoro variant of BTFMA possessed a chemical shift range of 1.07 ppm, showing that there is not a significant difference between using a difluoromethyl over a trifluoromethyl group.

BTFS, an analog to BTFA, had a chemical shift range of 1.21 ppm, suggesting that for non-aromatic systems, placing stronger EWGs can enhance the sensitivity of an adjacent CF_3 group. Interestingly, BTFP, which possess a weaker EWG than BTFS achieved a greater chemical shift range of 1.25 ppm. It is currently believed that the enhanced sensitivity being observed is due to solvation effects around the hydroxyl group. When placing two CF3 groups adjacent to each other we experienced a decrease in sensitivity, as seen in, 1,1,1,3,3,3-hexafluoro-2-methyl-2-propanol which has a chemical shift range of 0.94 ppm. Placing an adjacent EWG such as a phenyl ring also lead to a decrease in sensitivity, which is observed in 1,1,1,3,3,3-hexafluoro-2-phenyl-2-propanol, with a chemical shift range of 0.82 ppm (Figure 3-10). Although BTFP provided a substantial increase in sensitivity, by having a chiral center it can pose a potential issue when labeling, in which, if the tag is held in place it could lead to two sets up peaks corresponding to (S) or (R) stereochemistry. While 1,1,1,3,3,3-hexafluoro-2-methyl-2-propanol is slightly less sensitive compared to BTFMA, having a hexafluorinated species would allow for quicker experiments, or less protein being required for NMR due to increased signal intensity caused by the two CF_3 groups being equivalent.

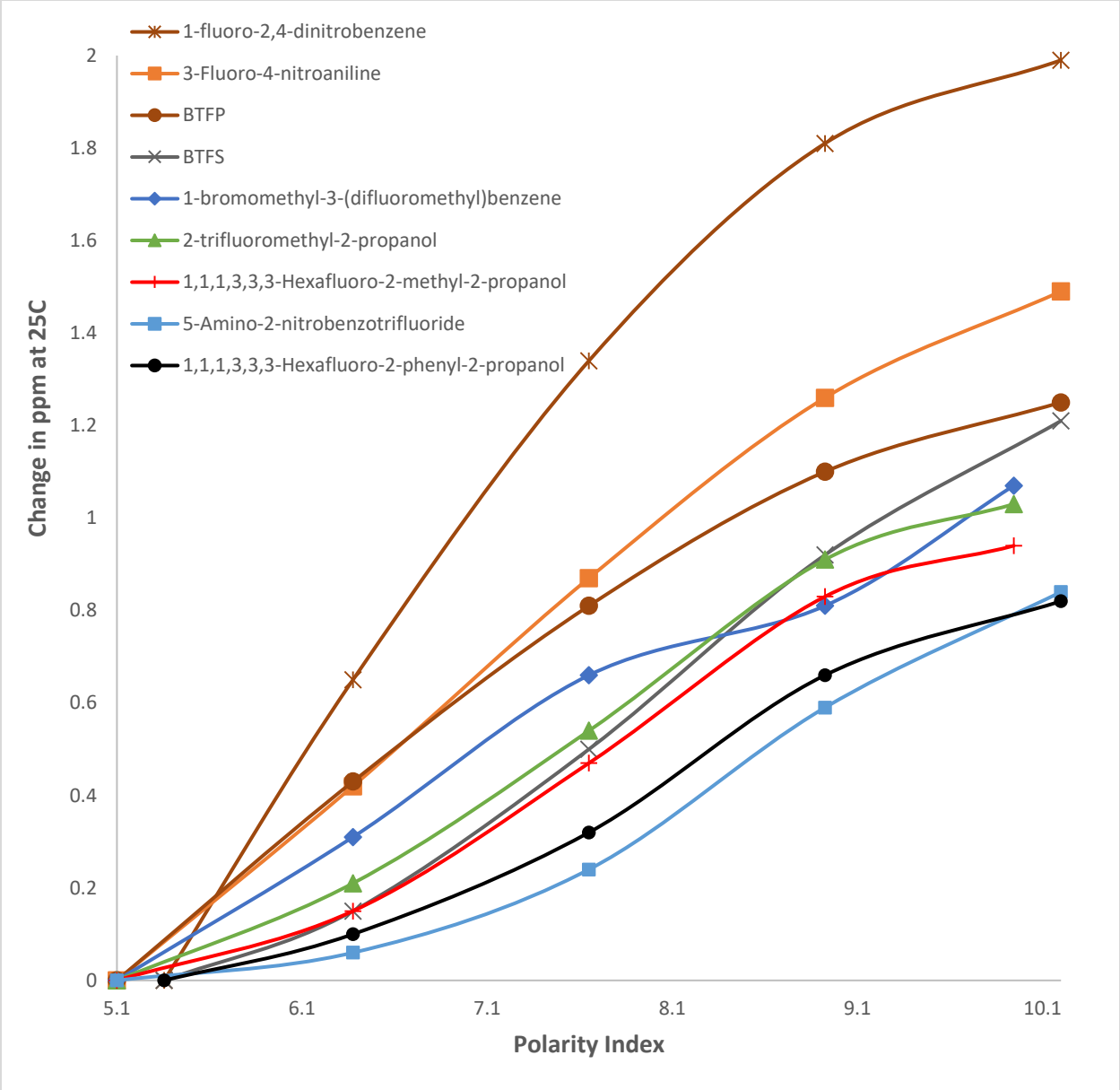

Figure 3-10 Summary of chemical shifts observed for various fluorinated compounds at 25°C. Solutions were made in various ratios of MeOH to H_2O, where a polarity index of 5.1 represents 100% MeOH and 10.2 is 100% H_2O.

3.3 Synthesis of New Thiol Specific Tags

Most of the small molecules tested were not functionalized for protein labeling. Efforts were put into functionalizing 6-TFHP, and 5-MFHP, which were the most sensitive to local environmental changes, to be thiol specific as most proteins do not natively contain free cysteine residues, thus the labeling sites can be controlled more effectively. Initially, an alkyl bromide functional group was used (6-TMeBr) as it was commercially available, and it was known to be thiol reactive. However, upon labeling it was determined to be reactive to both cysteine and methionine (Appendix 45-Appendix 46). BTFMA, on the hand, demonstrates selectivity for cysteine (Appendix 47-Appendix 48) under the same conditions. Thus, it was determined that using a bromo-acetamide group would allow for selectivity of cysteines. To modify the alkyl bromide into a bromo-acetamide it was reacted with methylamine, converting the alkyl bromide into a methylamine and then reacted with bromoacetyl bromide, forming a bromo-acetamide group (Figure 3-11). Upon modification to a bromo-acetamide group, 6-TBrA shows selectivity for cysteines (Appendix 49-Appendix 50).

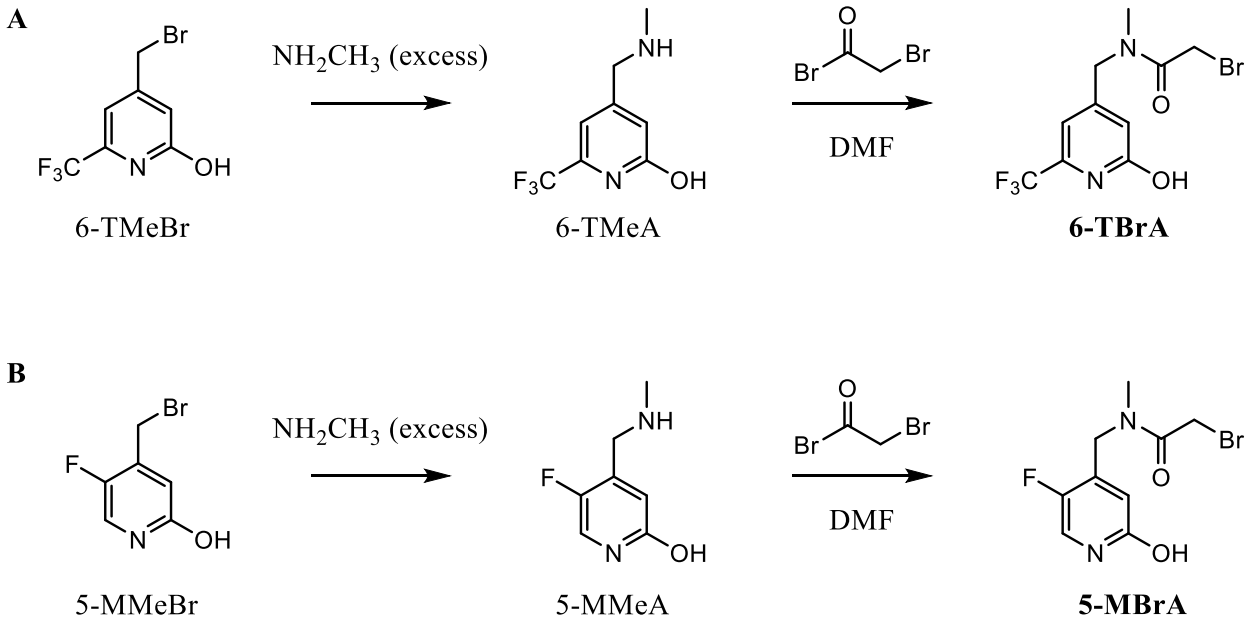

Figure 3-11 Synthetic scheme for functionalizing thiol specific tags.

3.4 Protein Labeling

The final stage of designing novel fluorinated tags is to test it on various protein systems. This should be done with simple proteins which have transition states from inactive to active upon addition of a ligand. Protein labeling was done using G-αS-Y358C provided by Shuya (Kate) Huang. The alpha subunit of the G-protein is moderately stable alone but more importantly is anticipated to adopt distinct conformations when nucleotide-free or bound to GDP, GTP-γS, or AlF4 with GDP and Mg^{2+}. Thus, depending on the labeling site, the G-protein can be used to test chemical shift sensitivity of specific fluorinated tags. The Y358C mutant is known to be situated in a pocket of the protein that is allosterically sensitive to the nucleotide or nucleotide analog.

BTFA and BTFMA were used as control groups for the newly functionalized tautomeric tags, 6-TBrA and 5-MBrA. Addition of GDP places the G-protein into a nucleotide bound state, when AlF_4 is added in addition to GDP and Mg^{2+} it adopts a similar conformation to GTPgS, and shifts the equilibrium into the G-protein's active state. Addition of GTPγS competes off the AlF_4, as well as, place it into its active state. BTFA, which is the least sensitive among the tags being examined, shows a chemical shift change of ~0.016 ppm between GDP bound and AlF_4 (or GTPγS) bound active states (Figure 3-12). BTFMA, the currently used tag for protein labeling, upon addition of AlF_4 show a chemical shift of ~0.16 ppm and slightly lower chemical shift for GTPγS of ~0.15 ppm, which could indicate that AlF_4 puts it into a slightly different active state than GTPγS (Figure 3-13).

5-MBrA, the newly synthesized monofluorinated species which had previously shown the largest chemicals shift range among all compounds tested, shows a chemical shift change of ~0.05 ppm from GDP to AlF_4, and from GDP to GTPγS it shows a shift of ~0.06 ppm. While this was not greater than BTFMA as expected, it does show another state in GTPγS which is separated by ~0.26 ppm to the right of the major peak (Figure 3-14). 6-TBrA, the trifluoromethyl species that was synthesized, shows the most interesting results. Two distinct peaks can be observed in each of the spectras. In GDP the two states are separated by ~0.08 ppm, in AlF_4 and GTPγS they are separated by ~0.13 ppm (Figure 3-15). The leading hypothesis is that population on the right represents a nucleotide free state, while the other is a nucleotide bound state. When we re-examined the spectra obtained with BTFMA, we observe an extremely broaden peak to the right which may correlate to the nucleotide free state. While the chemical shift changes are not as

great as in BTFMA for a single peak, it was able to show two distinct states which were not previously seen. Although, only one protein system has been currently surveyed the trifluoromethyl tag, 6-TBrA demonstrates promising results for other protein systems.

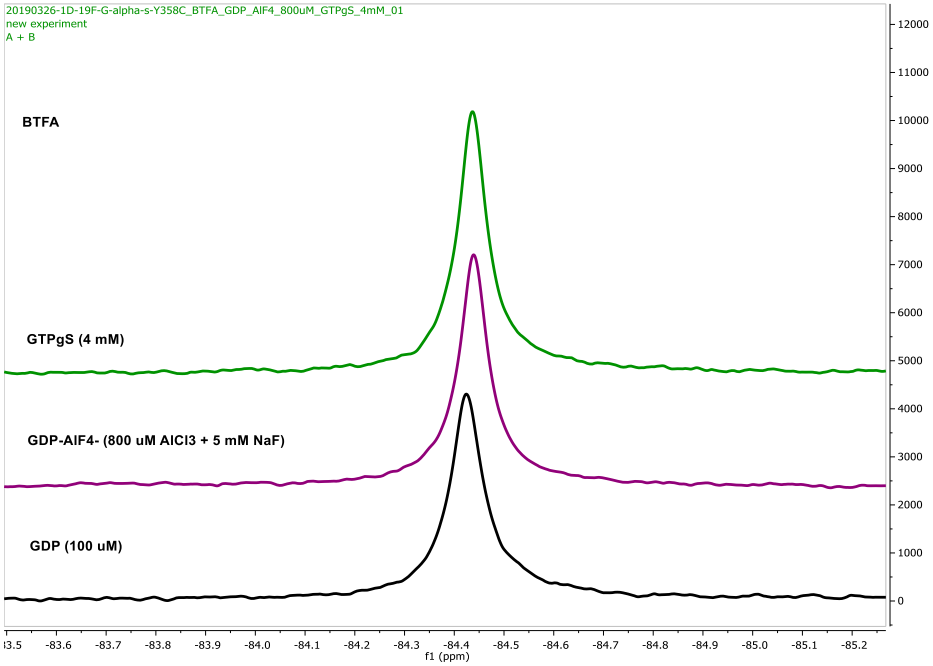

Figure 3-12 G-αS labeled with BTFA.

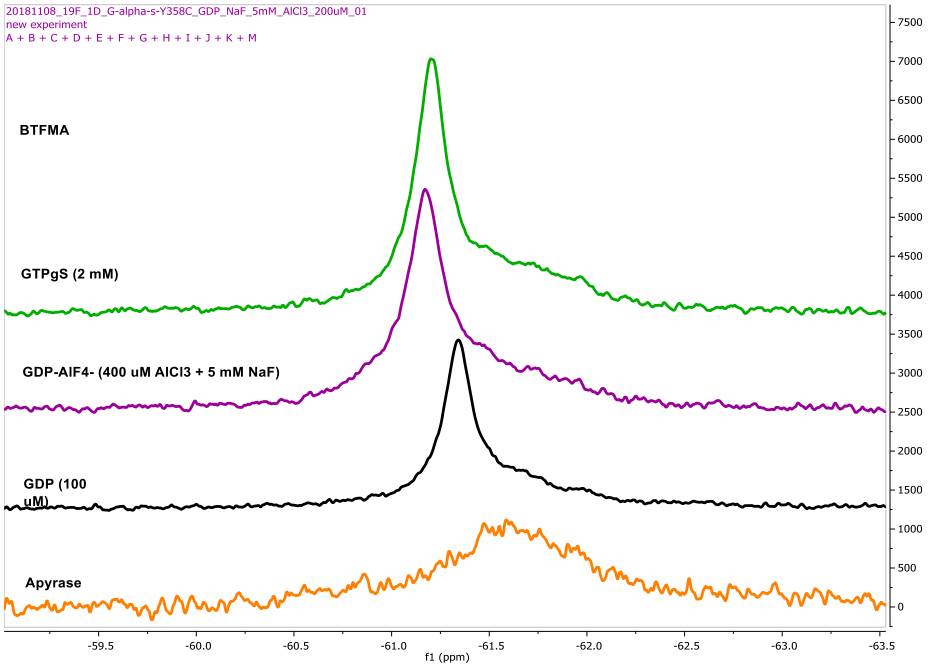

Figure 3-13 G-αS labeled with BTFMA.

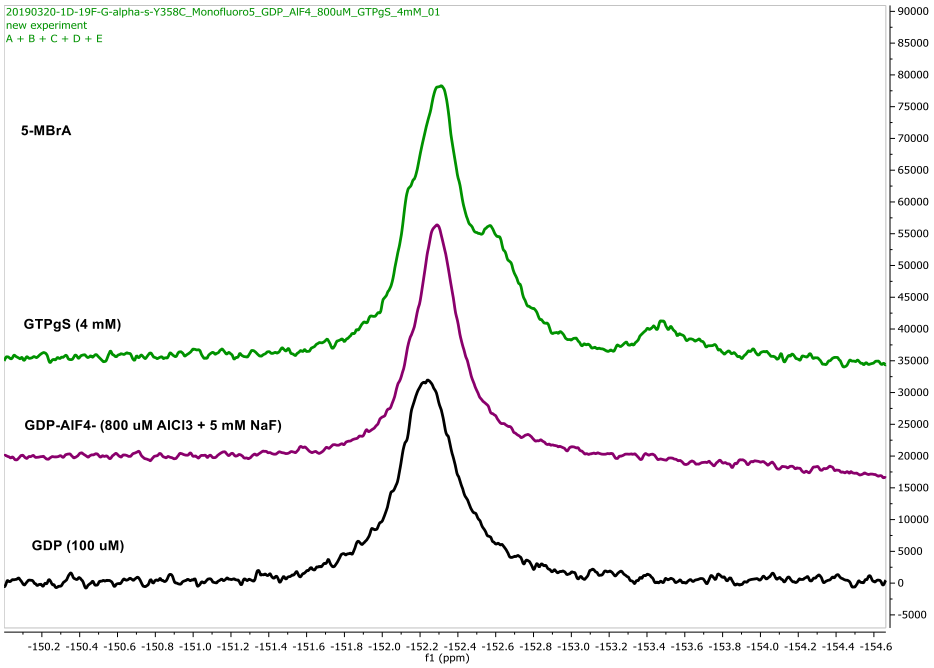

Figure 3-14 G-αS labeled with 5-MBrA.

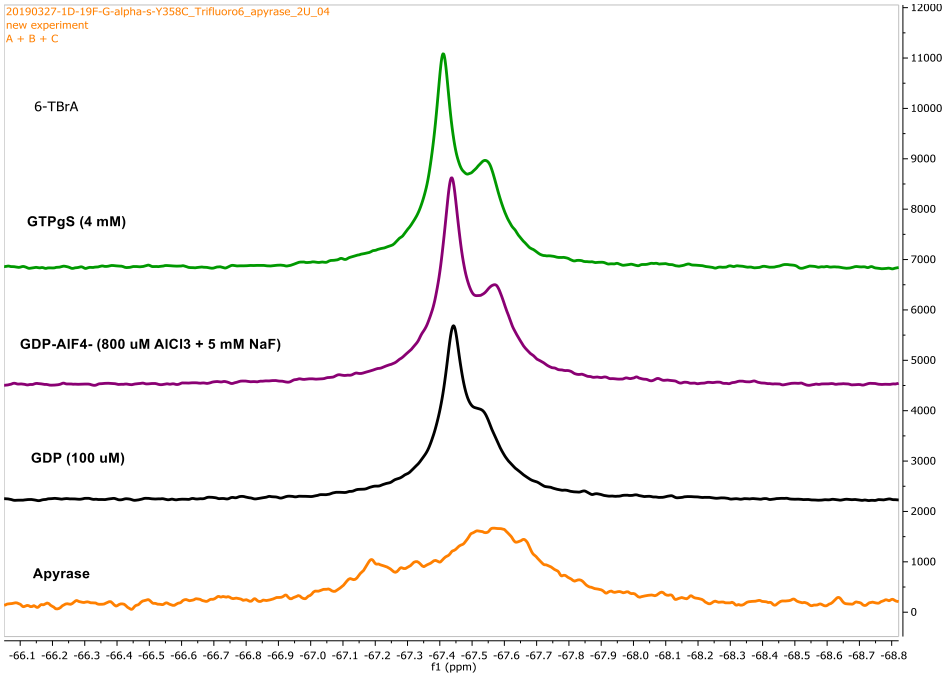

Figure 3-15 G-αS labeled with 6-TBrA.

Chapter 4

Conclusion

In protein studies involving structure and conformation states, 19F NMR can provide a great deal of insight into the local environment using a fluorinated tag. Enhancement of fluorine sensitivity through the use of tautomers and electronic effects can contribute to elucidation of protein conformations and function, as well as, conformational dynamics. This is illustrated by 5-MFHP and 6-TFHP where the combination of a polarizable aromatic, tautomeric equilibrium, and high sensitivity of the fluorine nuclei, gave rise to a wide range of chemical shifts with respects to changes in solvent polarity, temperature, and pH.

Through the numerous experiments conducted in this study, the pronounced sensitivity of the investigated compounds were revealed, demonstrating their viability for looking at subtle changes in polarity. As expected based on previous work by Ye *et al.* (2015) the polarizability and electron withdrawal in 6-TFHP were inferior to the monofluorinated species 5-MFHP.[3] The chemical shift range of 5-MFHP was 2.56 ppm which greater than that of 6-TFHP which was 1.61 ppm and considerably greater that of BTFMA which is at 1.03 ppm. However, the major drawback of the monofluorinated species is the signal is 1/3 that of an equivalent trifluoromethyl species which also exhibits longer T2 relaxation times (narrower line widths) in large proteins.

Functionalization of 6-TFHP and 5-MFHP into thiol specific tags using the same bromo-acetamide linking group as BTFMA proved to be successful. The protein labeling using G-αS demonstrated potential for being a more sensitive ^{19}F thiol specific tag, showing two distinct states in the case of 6-TBrA, and in 5-MBrA when treated with GTPγS, whereas in BTFMA we observe one distinct peak and another extremely broadened peak.

4.1 Future Directions

Although the data from the G-αS looks promising, more protein systems need to be tested in order to conclude if these next generation tags are actually performing as intended. Ideally, proteins that have simple opening and closing motions when given substrate and/or ligand, as this would provide a more reliable means of accessing the tags sensitivity. Maltose binding protein (MBP) and calmodulin would be good candidates for testing the sensitivity of ^{19}F thiol specific tags, as they adopt a rigid structure upon binding of ligand.[22-24]

Functionalization of the monofluoro tautomeric species 6-MFHP (Figure 4-1) could prove to be more optimal for registering conformational changes compared to 5-MBrA, given that it has similar sensitivity to 5-MFHP with a chemical shift range of 2.59 ppm and the fluoro group would be more solvent accessible.

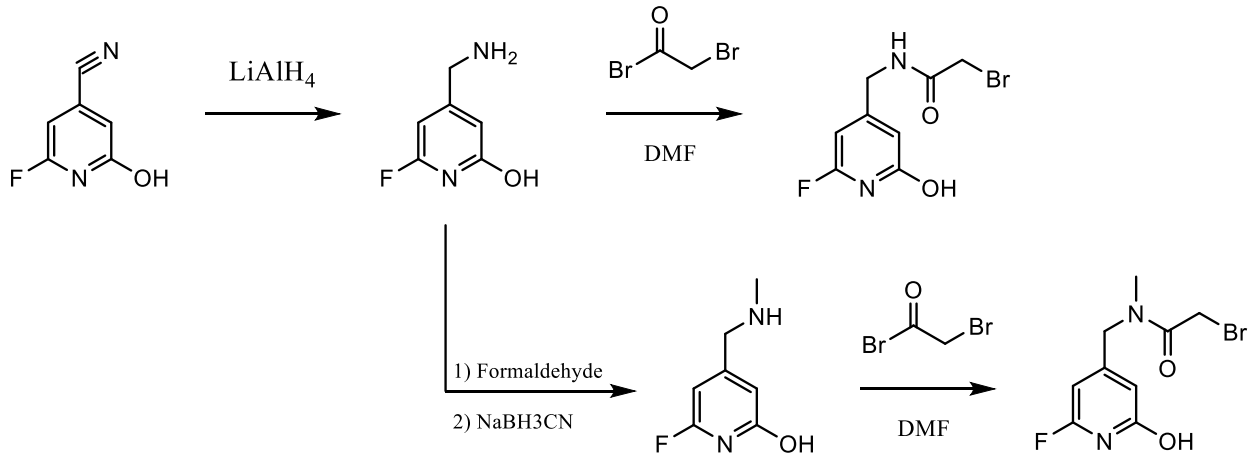

Figure 4-1 Proposed synthesis for functionalizing 6-MFHP into a thiol specific tag using commercially available starting material.

Further investigation and functionalization of the hexafluoro species (Figure 4-2) may lead to tag with chemical shift sensitivity that are on par with BTFMA but provide a substantial increase in signal intensity due to the presence of two CF3 groups. This would allow for short experiment run times, or less protein sample being required for NMR experiments.

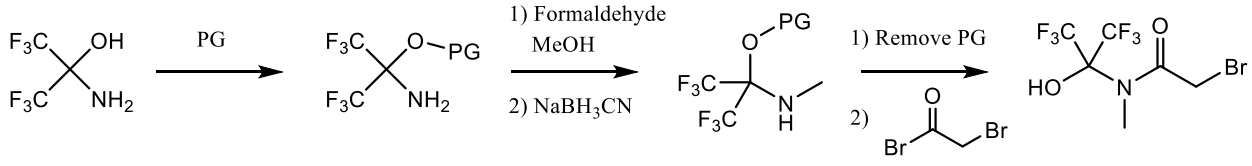

Figure 4-2 Proposed synthesis for functionalizing of a hexafluoro species into a thiol specific tag using commercially available starting material.

References

1. Günther H. *NMR spectroscopy: Basic principles, concepts and applications in chemistry.* Weinheim: Wiley-VCH; 2013.

2. Gouverneur V. *Guide to fluorine NMR for organic chemists. by william R. dolbier.* Vol 49. ; 2010:4335.

3. Ye L, Larda ST, Frank Li YF, Manglik A, Prosser RS. A comparison of chemical shift sensitivity of trifluoromethyl tags: Optimizing resolution in ^{19}F NMR studies of proteins. *J Biomol NMR*. 2015;62(1):97-103.

4. Sloop J. 19-fluorine nuclear magnetic resonance chemical shift variability in trifluoroacetyl species. *Reports in Organic Chemistry*. 2013;3:1-12.

5. Purser S, Moore PR, Swallow S, Gouverneur V. Fluorine in medicinal chemistry. *Chem Soc Rev*. 2008;37(2):320-330.

6. Chambers RD. *Fluorine in organic chemistry.* Oxford [u.a.]: Blackwell [u.a.]; 2004.

7. Didenko T, Liu JJ, Horst R, Stevens RC, Wüthrich K. Fluorine-19 NMR of integral membrane proteins illustrated with studies of GPCRs. *Curr Opin Struct Biol*. 2013;23(5):740-747.

8. Crowley PB, Kyne C, Monteith WB. Simple and inexpensive incorporation of 19F-tryptophan for protein NMR spectroscopy. *Chemical communications (Cambridge, England)*. 2012;48(86):10681.

9. Liu JJ, Horst R, Katritch V, Stevens RC, Wüthrich K. Biased signaling pathways in β_2-adrenergic receptor characterized by ^{19}F-NMR. *Science*. 2012;335(6072):1106.

10. Kim TH, Chung KY, Manglik A, et al. The role of ligands on the equilibria between functional states of a G protein-coupled receptor. *Journal of the American Chemical Society*. 2013;135(25):9465-9474.

11. Kitevski-LeBlanc JL, Prosser RS. Current applications of 19F NMR to studies of protein structure and dynamics. *Prog Nucl Magn Reson Spectrosc*. 2012;62:1-33.

12. Chary KVR, Govil G. *NMR in biological systems: From molecules to human.* Springer Netherlands; 2008.

13. Pearson JG, Oldfield E, Lee FS, Warshel A. Chemical shifts in proteins: A shielding trajectory analysis of the fluorine nuclear magnetic resonance spectrum of the escherichia coli galactose binding protein using a multipole shielding polarizability-local reaction field-molecular dynamics approach. *Advanced Ceramic Materials*. 1993;115(15):6851-6862.

14. Lau EY, Gerig JT. Origins of fluorine NMR chemical shifts in fluorine-containing proteins. *Journal of the American Chemical Society*. 2000;122(18):4408-4417.

15. Jackson JC, Hammill JT, Mehl RA. Site-specific incorporation of a (19)F-amino acid into proteins as an NMR probe for characterizing protein structure and reactivity. *J Am Chem Soc*. 2007;129(5):1160-1166.

16. Li C, Wang G, Wang Y, et al. Protein 19F NMR in escherichia coli. *J Am Chem Soc*. 2010;132(1):321.

17. Sloop JC, Churley M, Guzman A, et al. Synthesis and reactivity of fluorinated cyclic ketones: Initial findings. *American Journal of Organic Chemistry*. 2014;4(1):1-10.

18. Antonov L. *Tautomerism.* Weinheim: Wiley-VCH; 2014.

19. Smith M, March J. *March's advanced organic chemistry: Reactions, mechanisms, and structure.* Hoboken, N.J: Wiley-Interscience; 2007.

20. Abraham RJ, Canton M, Reid M, Griffiths L. ChemInform abstract: Proton chemical shifts in NMR. part 14. proton chemical shifts, ring currents and π electron effects in condensed aromatic hydrocarbons and substituted benzenes. *ChemInform.* 2000;31(29):no.

21. Peng CS, Baiz CR, Tokmakoff A. Direct observation of ground-state lactam–lactim tautomerization using temperature-jump transient 2D IR spectroscopy. *PNAS.* 2013;110(23):9243-9248.

22. Sharff AJ, Rodseth LE, Spurlino JC, Quiocho FA. Crystallographic evidence of a large ligand-induced hinge-twist motion between the two domains of the maltodextrin binding protein involved in active transport and chemotaxis. *Biochemistry*. 1992;31(44):10657-10663.

23. Spurlino JC, Lu GY, Quiocho FA. The 2.3-A resolution structure of the maltose- or maltodextrin-binding protein, a primary receptor of bacterial active transport and chemotaxis. *J Biol Chem*. 1991;266(8):5202-5219.

24. Chou JJ, Li S, Klee CB, Bax A. Solution structure of ca(2+)-calmodulin reveals flexible hand-like properties of its domains. *Nat Struct Biol*. 2001;8(11):990-997.

Appendices

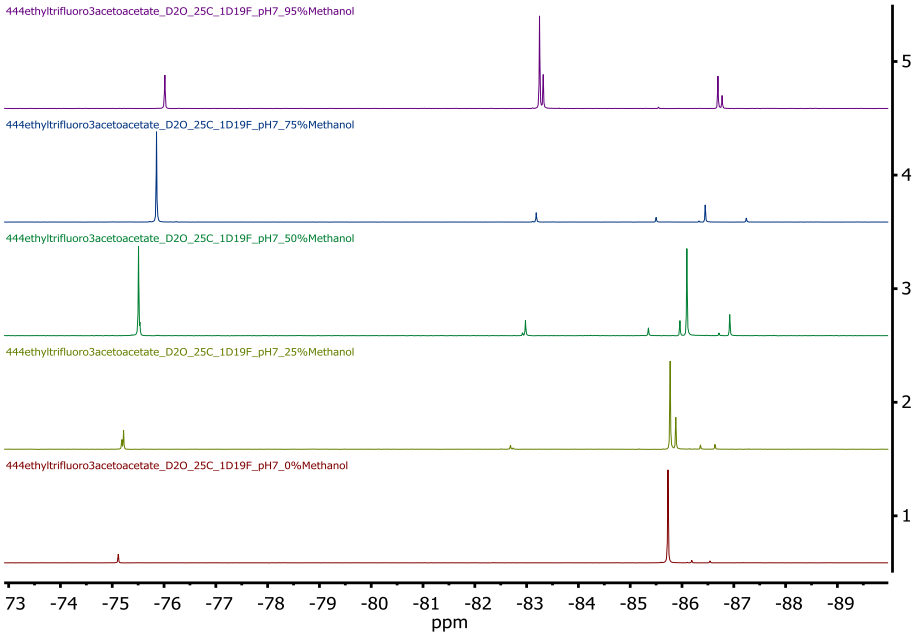

Appendix 1 1D ^{19}F spectra of ethyl 4,4,4-trifluoroacetoacetate with decreasing polarity (0-95% Water:Methanol) at 25°C.

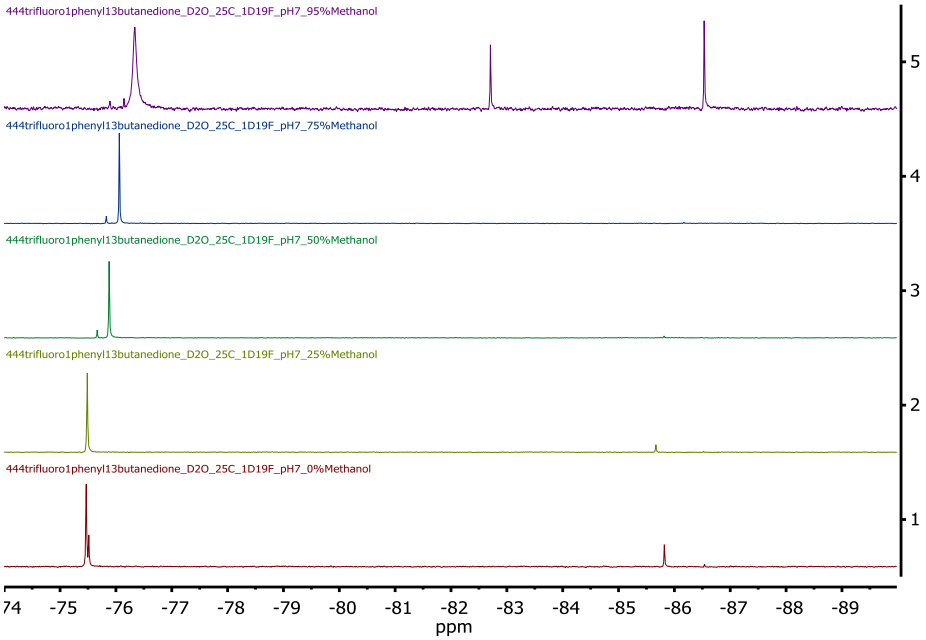

Appendix 2 1D ^{19}F spectra of 4,4,4-trifluoro-1-phenyl-1,3-butanedione with decreasing polarity (0-95% Water:Methanol) at 25°C.

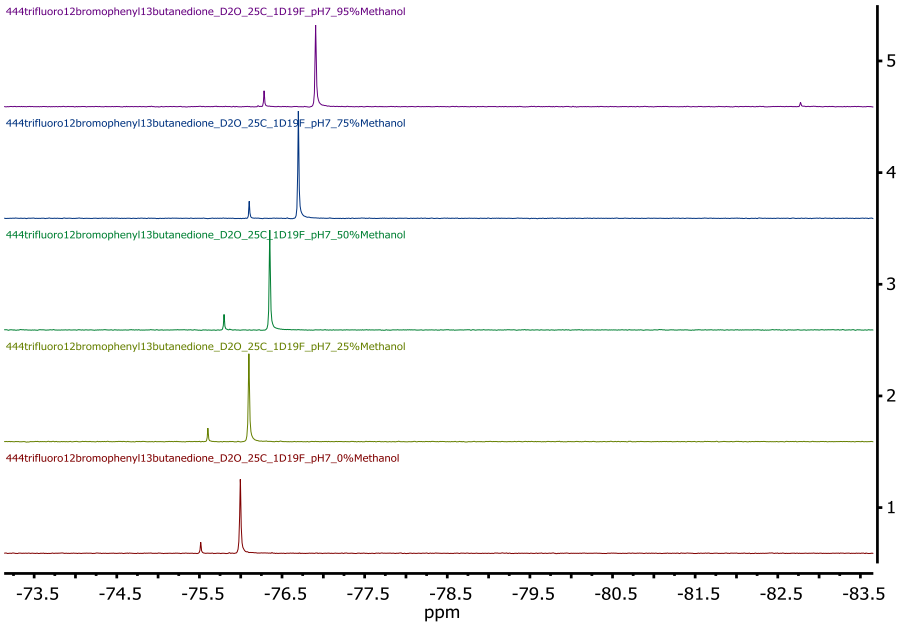

Appendix 3 1D ^{19}F spectra of 4,4,4-trifluoro-1-(2-bromophenyl)-1,3-butanedione with decreasing polarity (0-95% Water:Methanol) at 25°C.

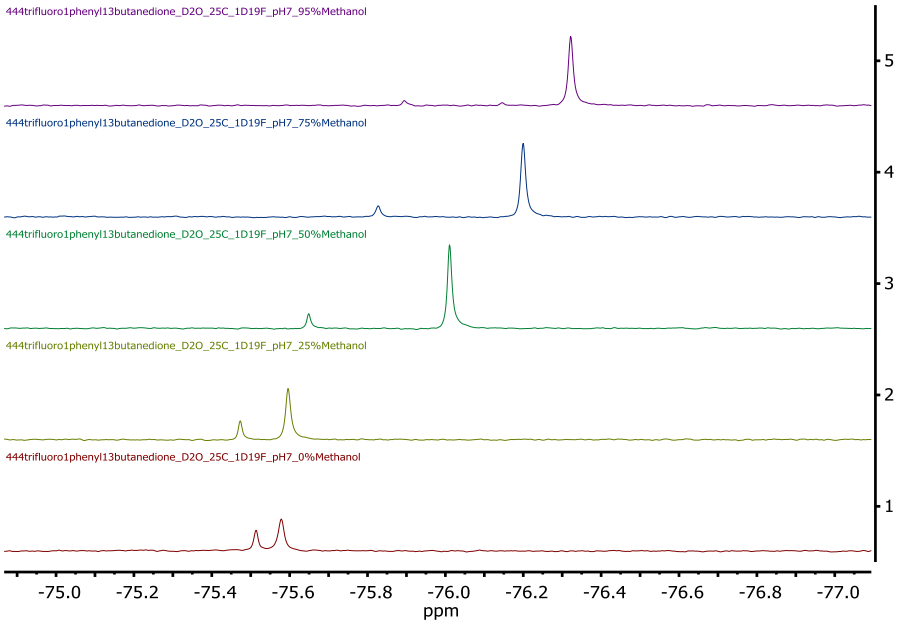

Appendix 4 1D ^{19}F spectra of 4,4,4-trifluoro-1-(3-bromophenyl)-1,3-butanedione with decreasing polarity (0-95% Water:Methanol) at 25°C.

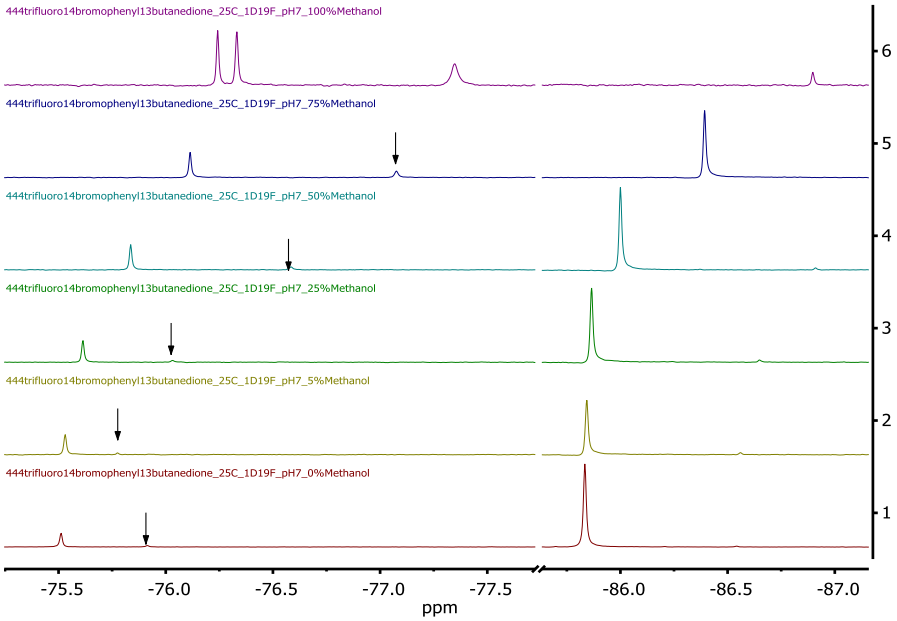

Appendix 5 1D ^{19}F spectra of 4,4,4-trifluoro-1-(4-bromophenyl)-1,3-butanedione with decreasing polarity (0-100% Water:Methanol) at 25ºC.

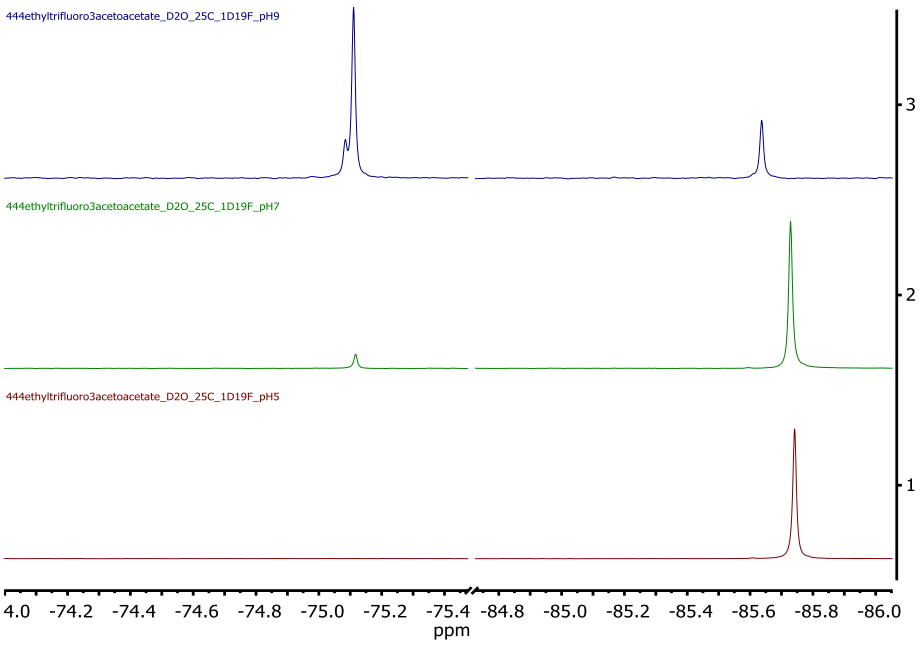

Appendix 6 1D ^{19}F spectra of ethyl 4,4,4-trifluoroacetoacetate with increasing pH (5-9) at 25ºC.

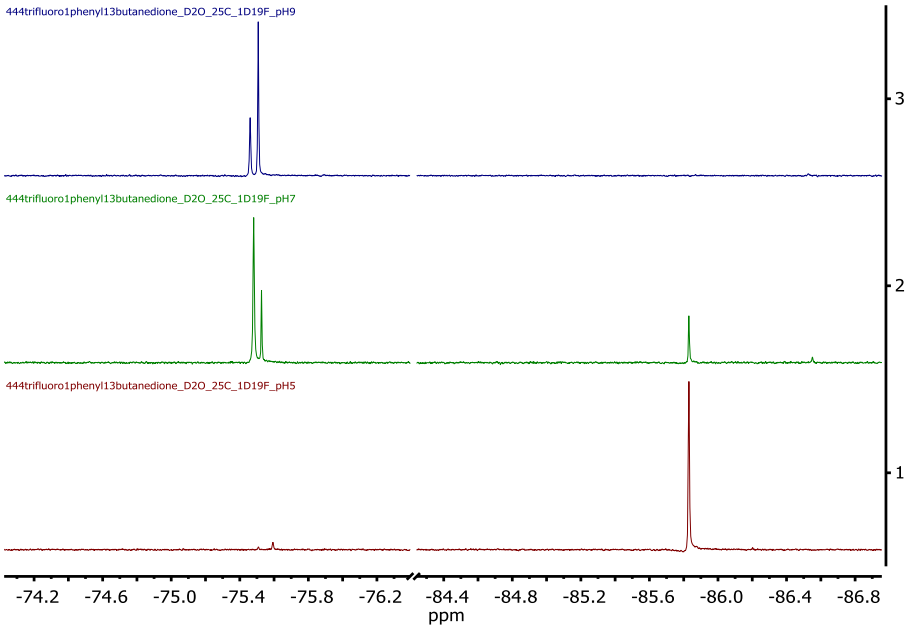

Appendix 7 1D ^{19}F spectra of ethyl 4,4,4-trifluoro-1-phenyl-1,3-butanedione with increasing pH (5-9) at 25ºC.

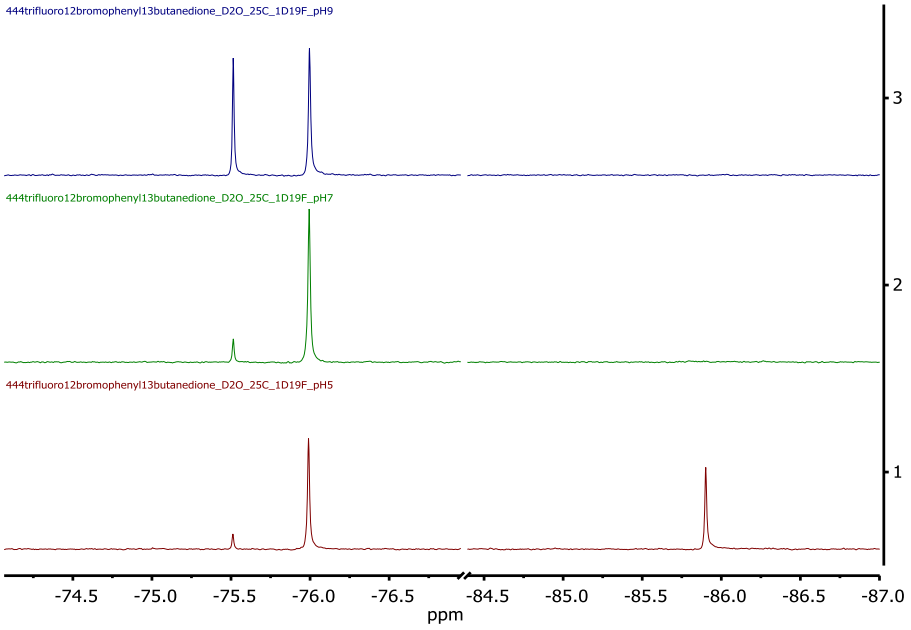

Appendix 8 1D ^{19}F spectra of 4,4,4-trifluoro-1-(2-bromophenyl)-1,3-butanedione with increasing pH (5-9) at 25ºC.

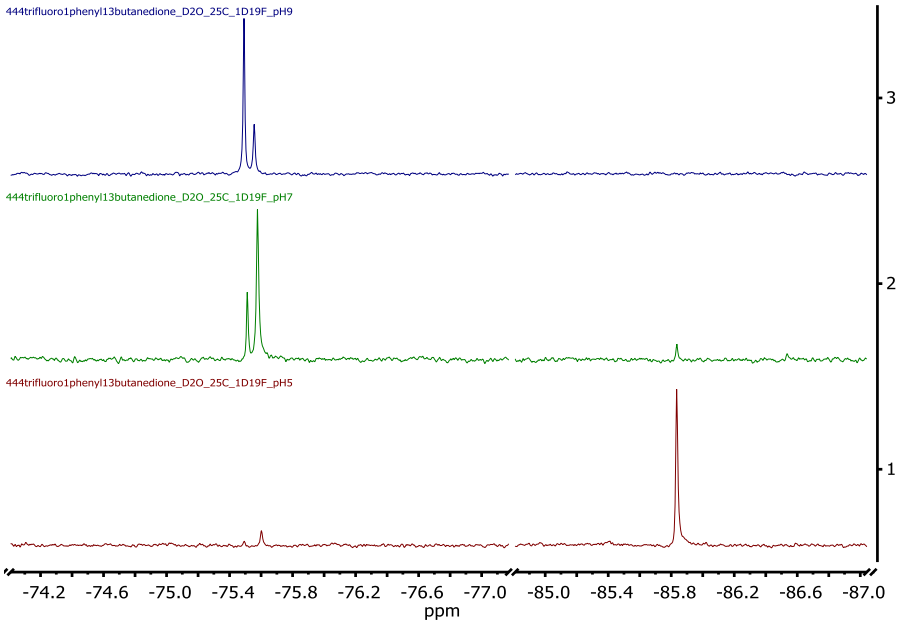

Appendix 9 1D ^{19}F spectra of 4,4,4-trifluoro-1-(3-bromophenyl)-1,3-butanedione with increasing pH (5-9) at 25ºC.

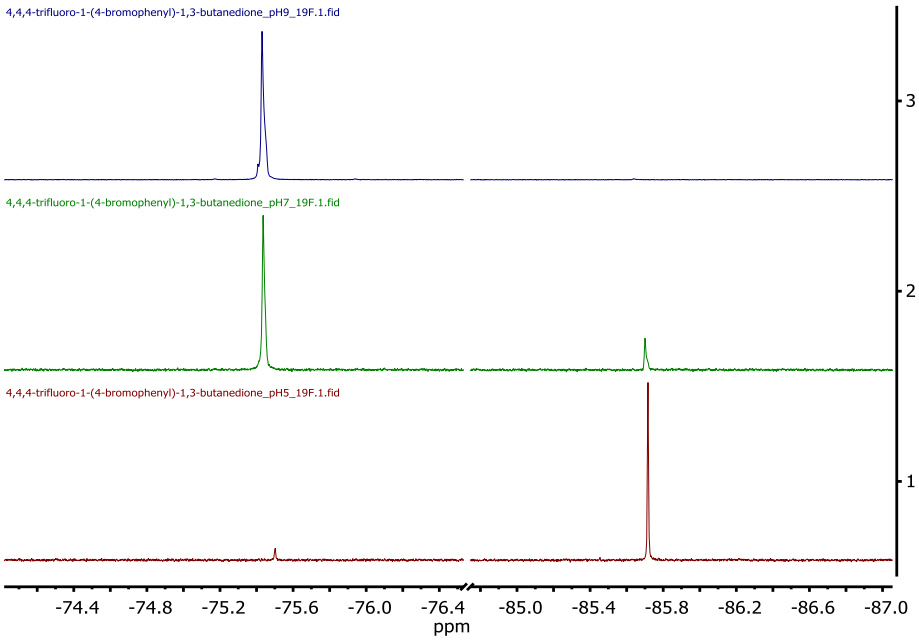

Appendix 10 1D ^{19}F spectra of 4,4,4-trifluoro-1-(4-bromophenyl)-1,3-butanedione with increasing pH (5-9) at 25ºC.

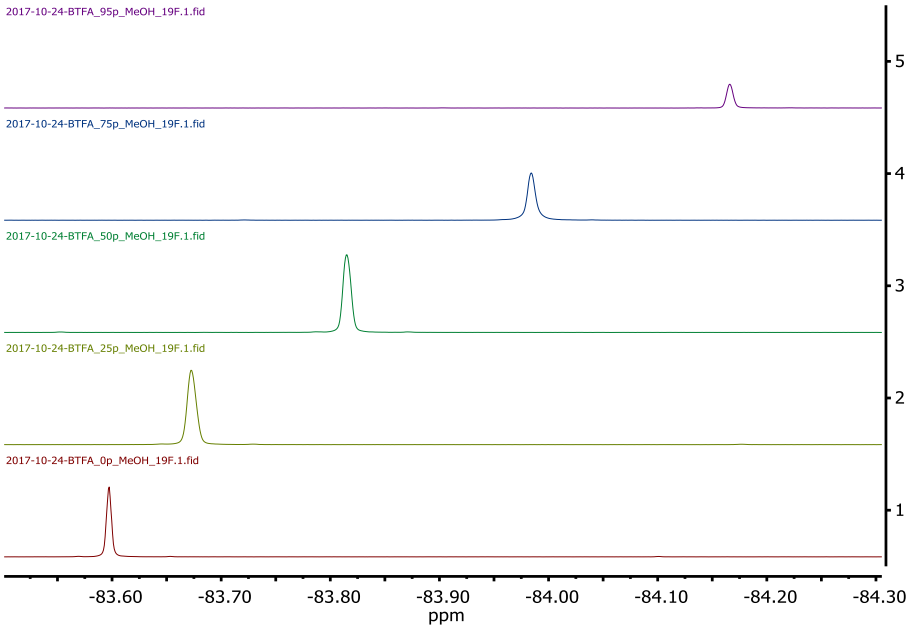

Appendix 11 1D ^{19}F spectra of BTFA with decreasing polarity (0-100% Water:Methanol) at 25ºC.

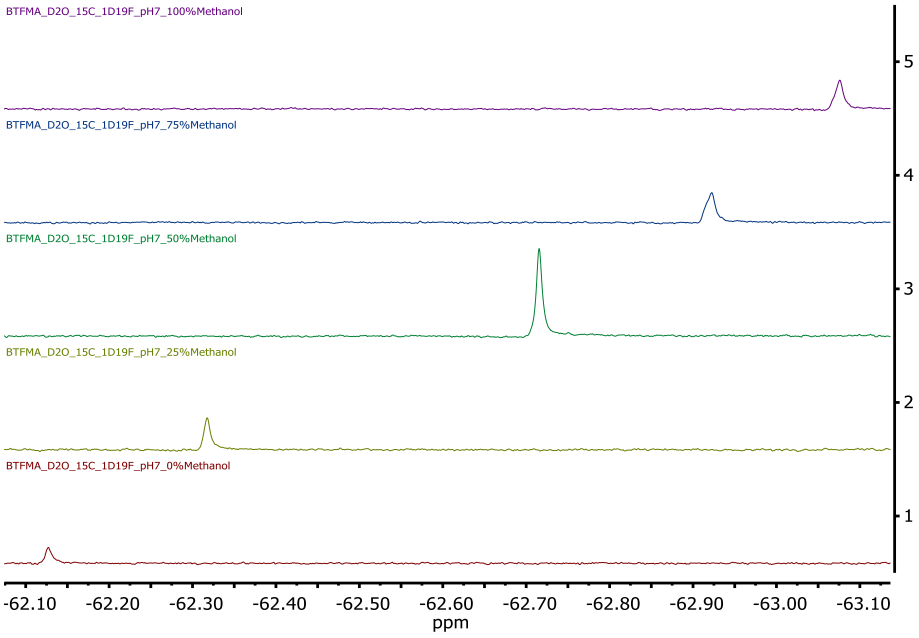

Appendix 12 1D ^{19}F spectra of BTFMA with decreasing polarity (0-100% Water:Methanol) at 15ºC.

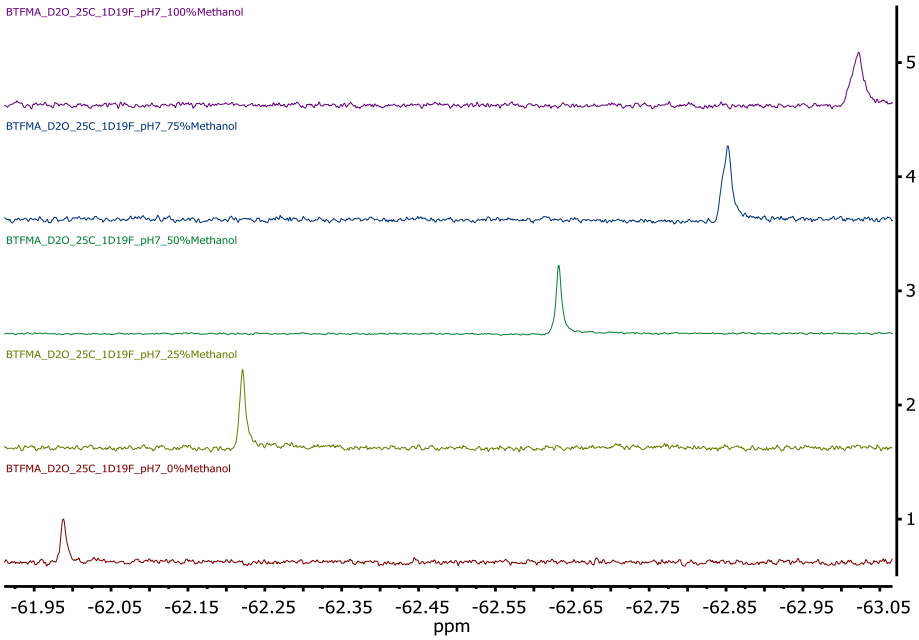

Appendix 13 1D ^{19}F spectra of BTFMA with decreasing polarity (0-100% Water:Methanol) at 25ºC.

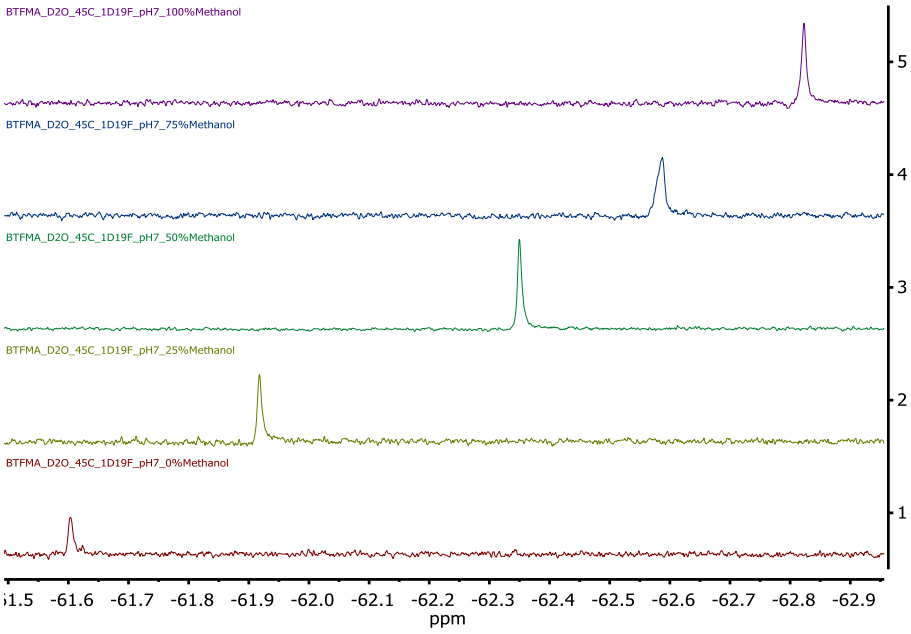

Appendix 14 1D ^{19}F spectra of BTFMA with decreasing polarity (0-100% Water:Methanol) at 45ºC.

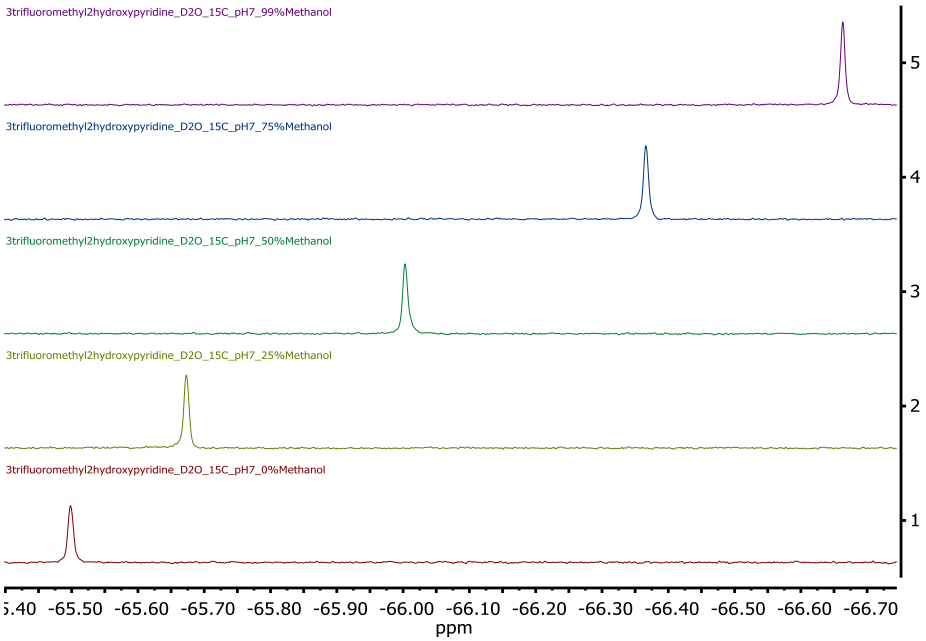

Appendix 15 1D ^{19}F spectra of 3-TFHP with decreasing polarity (0-99% Water:Methanol) at 15ºC.

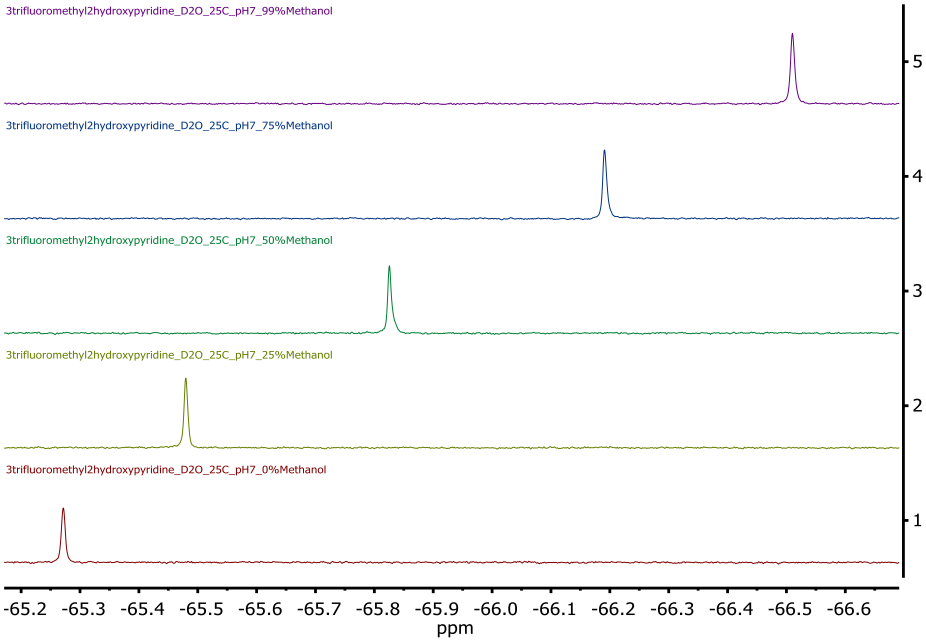

Appendix 16 1D ^{19}F spectra of 3-TFHP with decreasing polarity (0-99% Water:Methanol) at 25ºC.

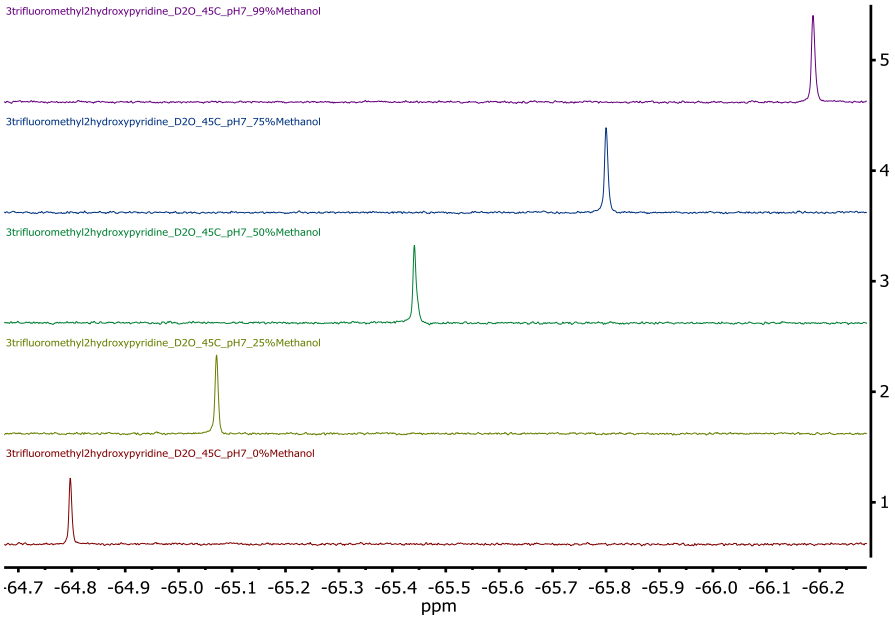

Appendix 17 1D ^{19}F spectra of 3-TFHP with decreasing polarity (0-99% Water:Methanol) at 45ºC.

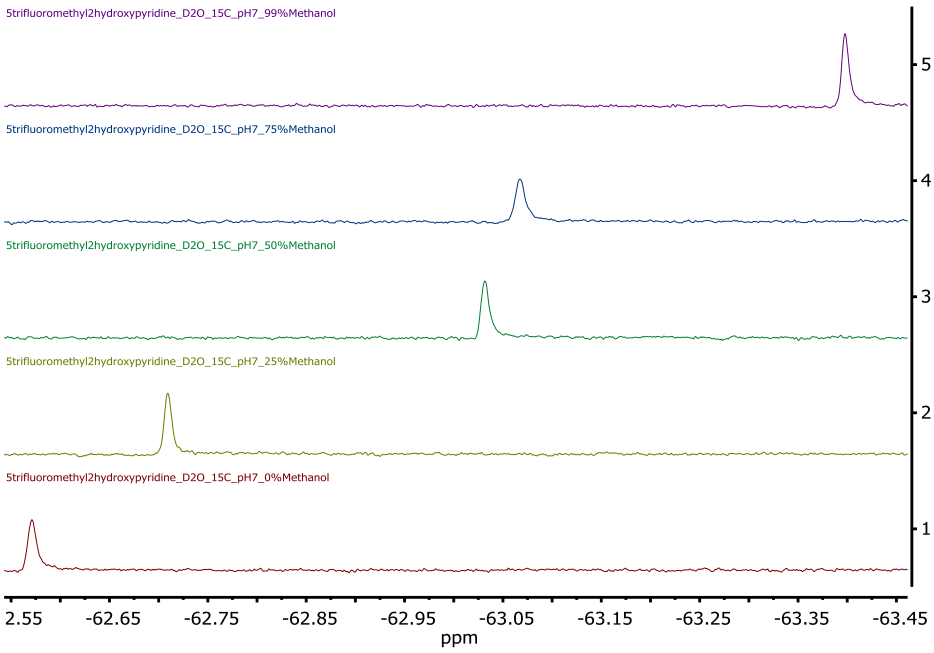

Appendix 18 1D ^{19}F spectra of 5-TFHP with decreasing polarity (0-99% Water:Methanol) at 15ºC.

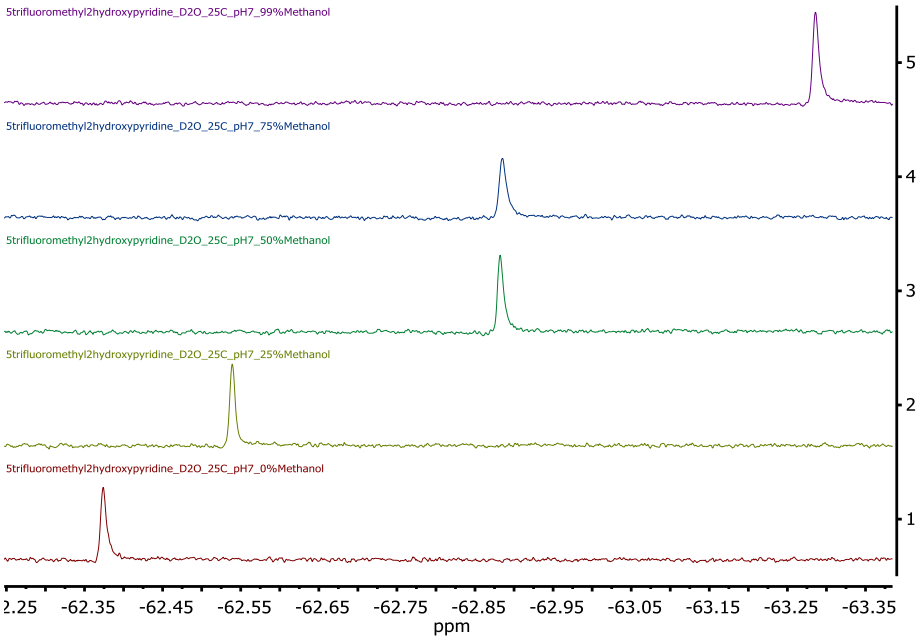

Appendix 19 1D ^{19}F spectra of 5-TFHP with decreasing polarity (0-99% Water:Methanol) at 25ºC.

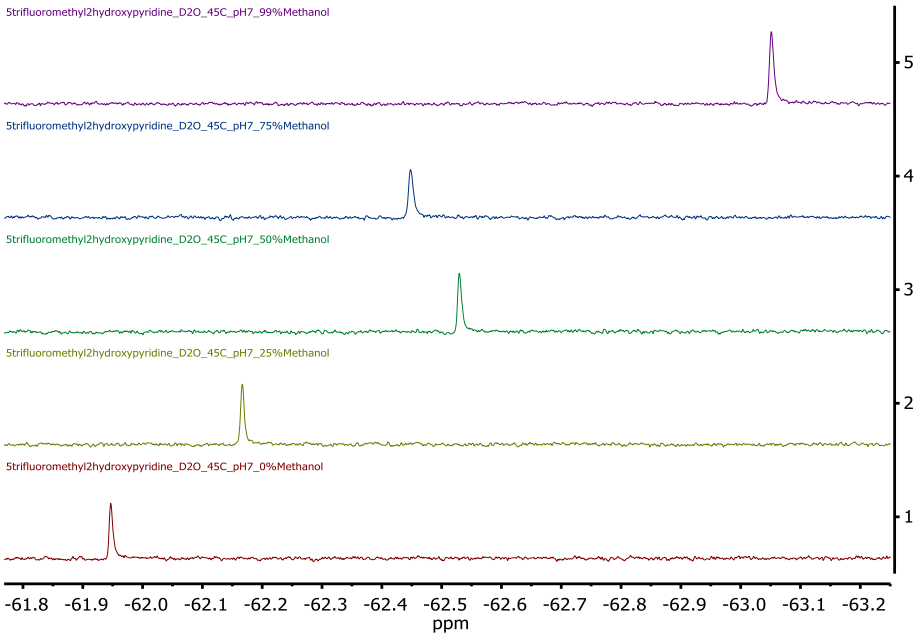

Appendix 20 1D ^{19}F spectra of 5-TFHP with decreasing polarity (0-99% Water:Methanol) at 45ºC.

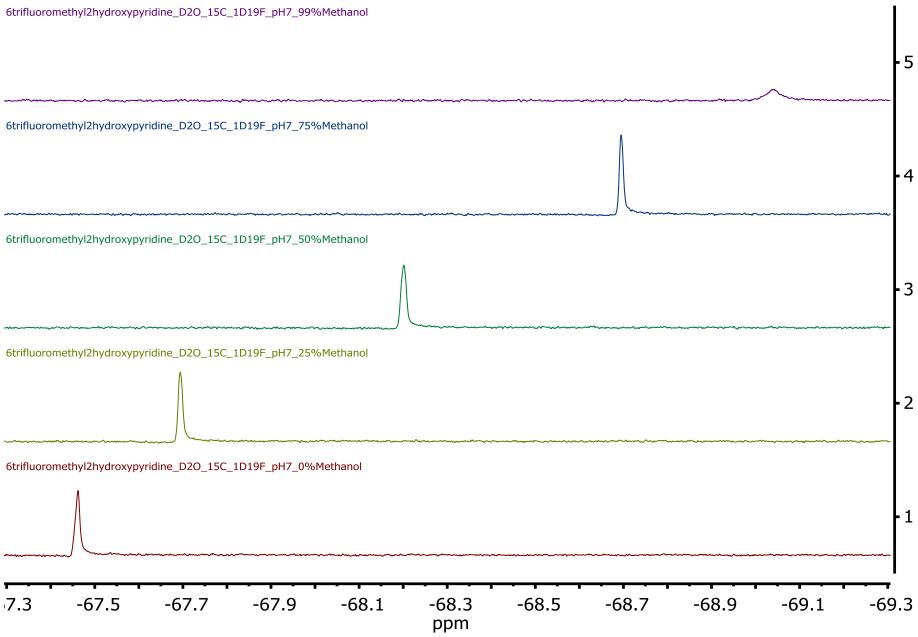

Appendix 21 1D ^{19}F spectra of 6-TFHP with decreasing polarity (0-99% Water:Methanol) at 15ºC.

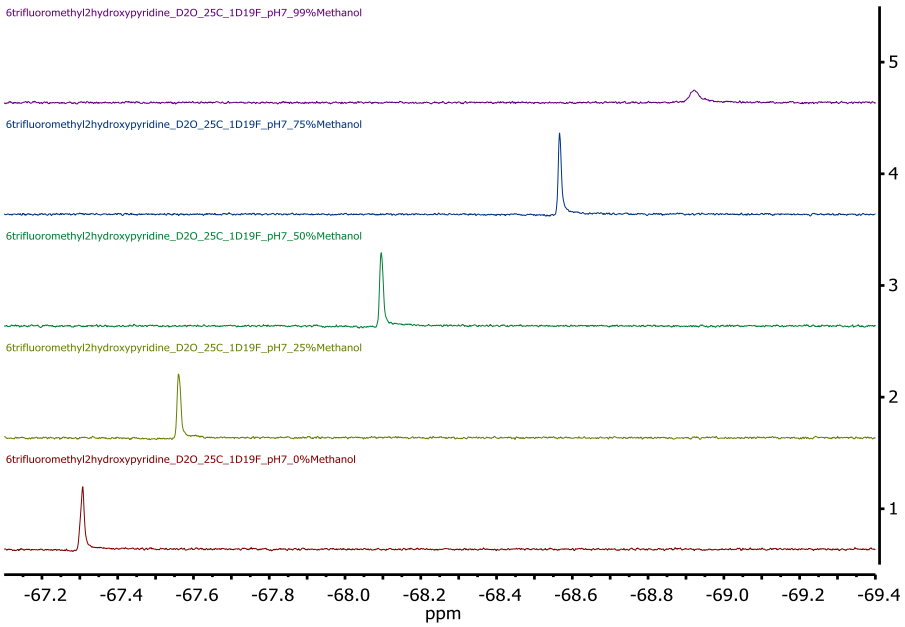

Appendix 22 1D ^{19}F spectra of 6-TFHP with decreasing polarity (0-99% Water:Methanol) at 25ºC.

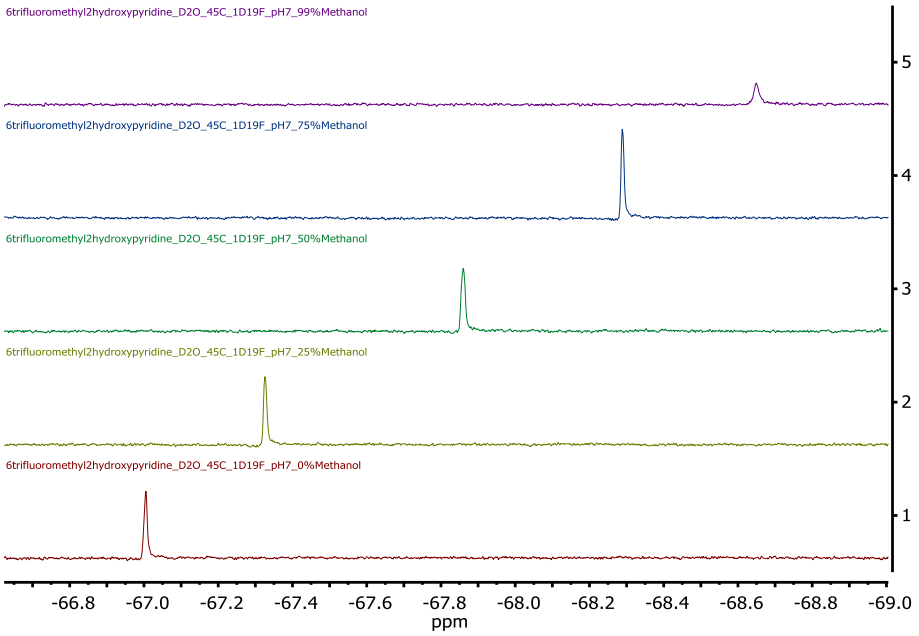

Appendix 23 1D ^{19}F spectra of 6-TFHP with decreasing polarity (0-99% Water:Methanol) at 45ºC.

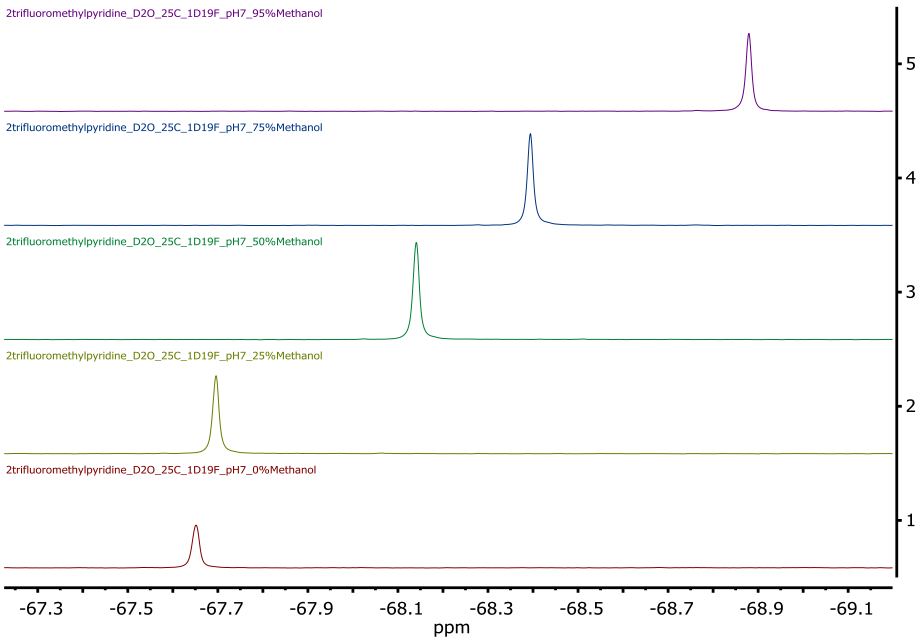

Appendix 24 1D ^{19}F spectra of 2-TFP with decreasing polarity (0-95% Water:Methanol) at 25ºC.

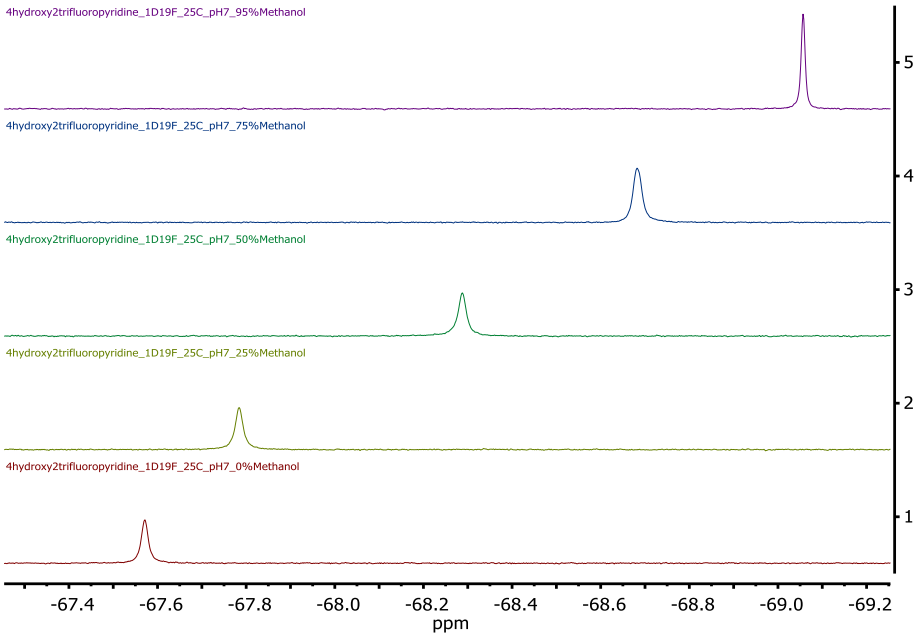

Appendix 25 1D ^{19}F spectra of 2-TF-4-HP with decreasing polarity (0-95% Water:Methanol) at 25ºC.

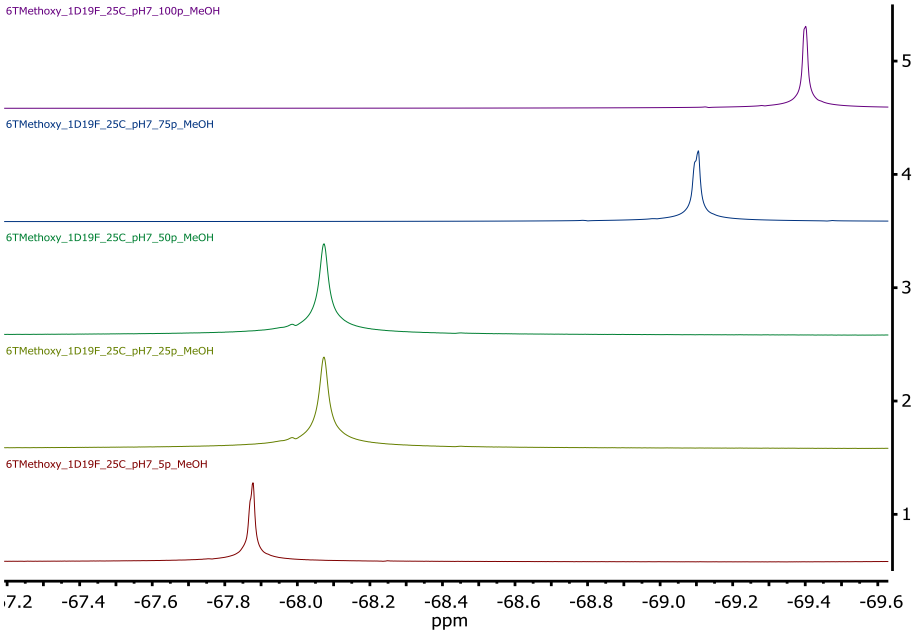

Appendix 26 1D ^{19}F spectra of 6-TFMP with decreasing polarity (5-100% Water:Methanol) at 25ºC.

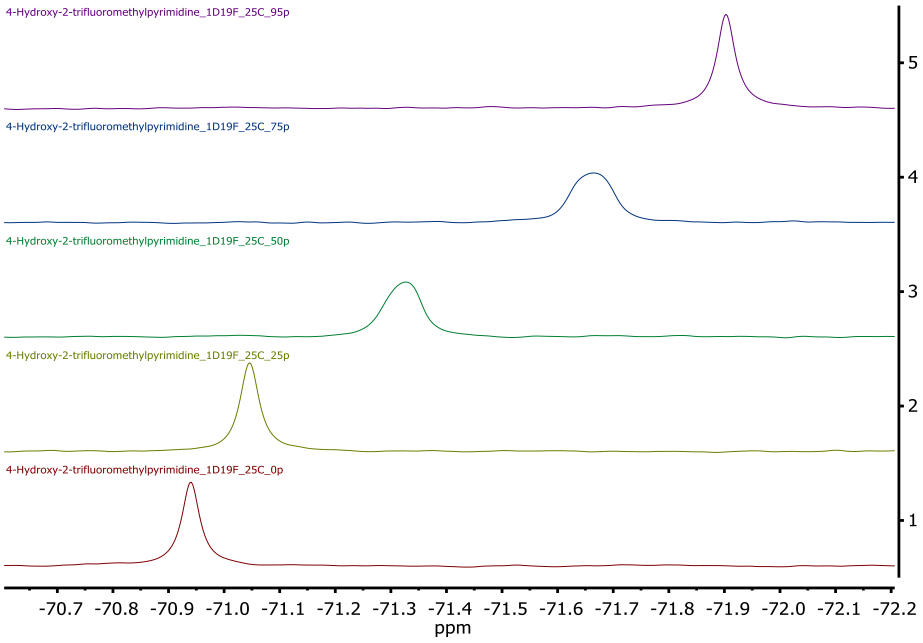

Appendix 27 1D ^{19}F spectra of 6-TFHPy with decreasing polarity (0-95% Water:Methanol) at 25°C.

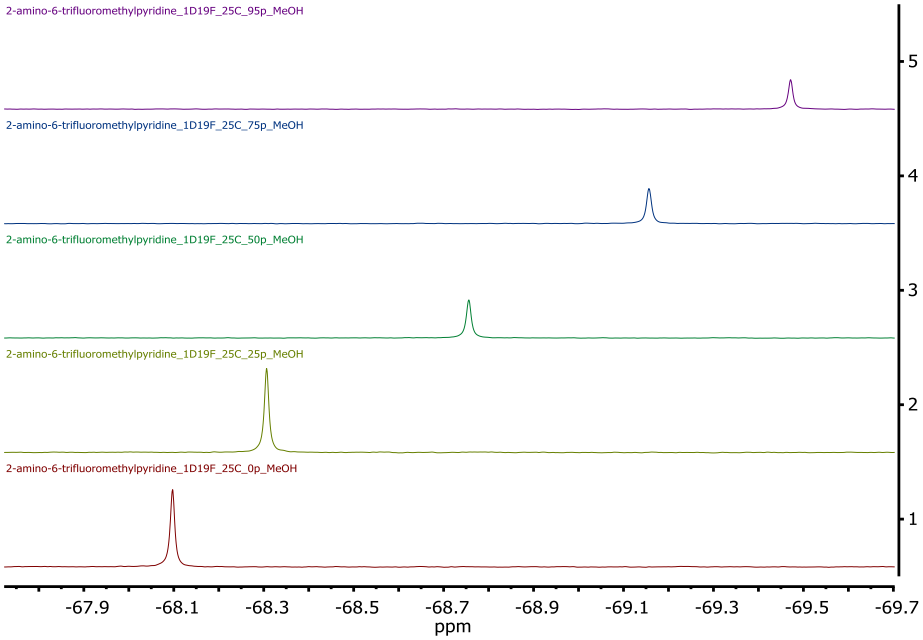

Appendix 28 1D ^{19}F spectra of 6-TFAP with decreasing polarity (0-95% Water:Methanol) at 25°C.

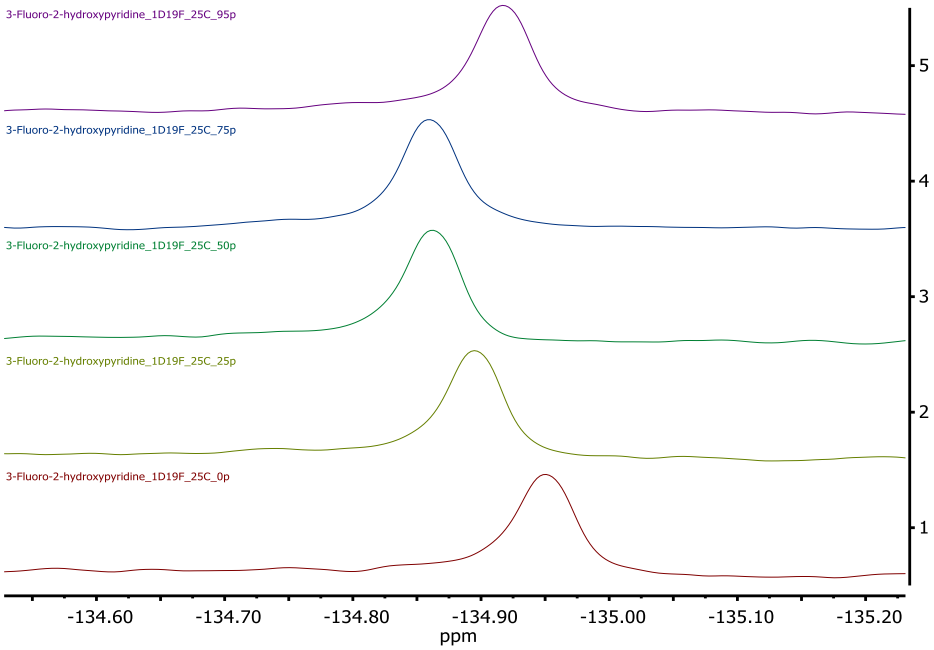

Appendix 29 1D ^{19}F spectra of 3-MFHP with decreasing polarity (0-95% Water:Methanol) at 25ºC.

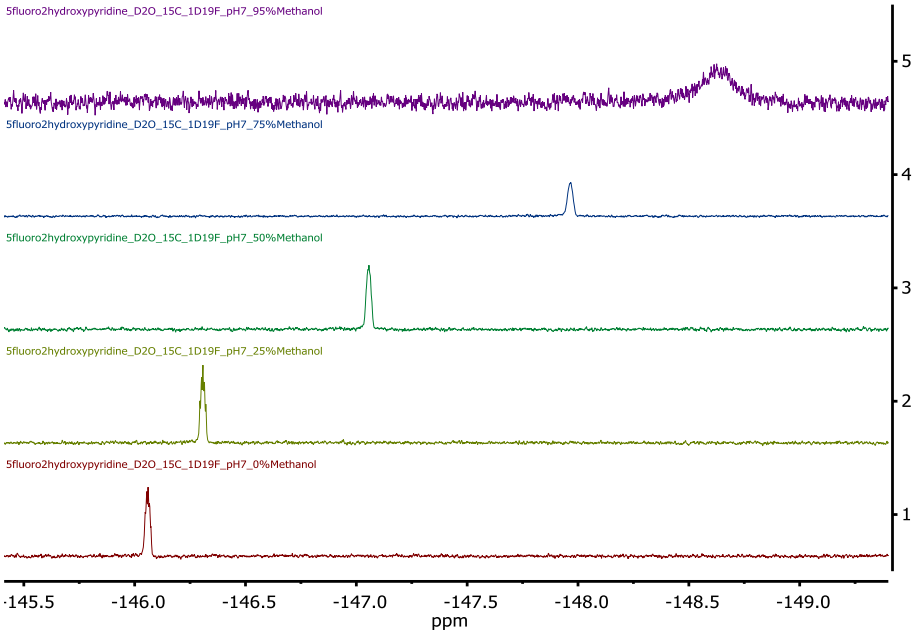

Appendix 30 1D ^{19}F spectra of 5-MFHP with decreasing polarity (0-95% Water:Methanol) at 15ºC.

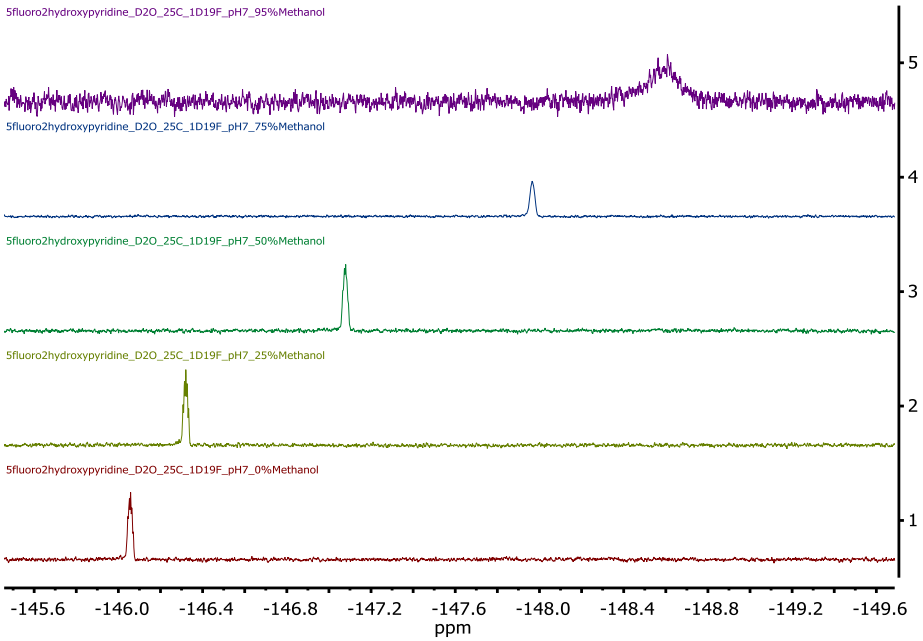

Appendix 31 1D ^{19}F spectra of 5-MFHP with decreasing polarity (0-95% Water:Methanol) at 25°C.

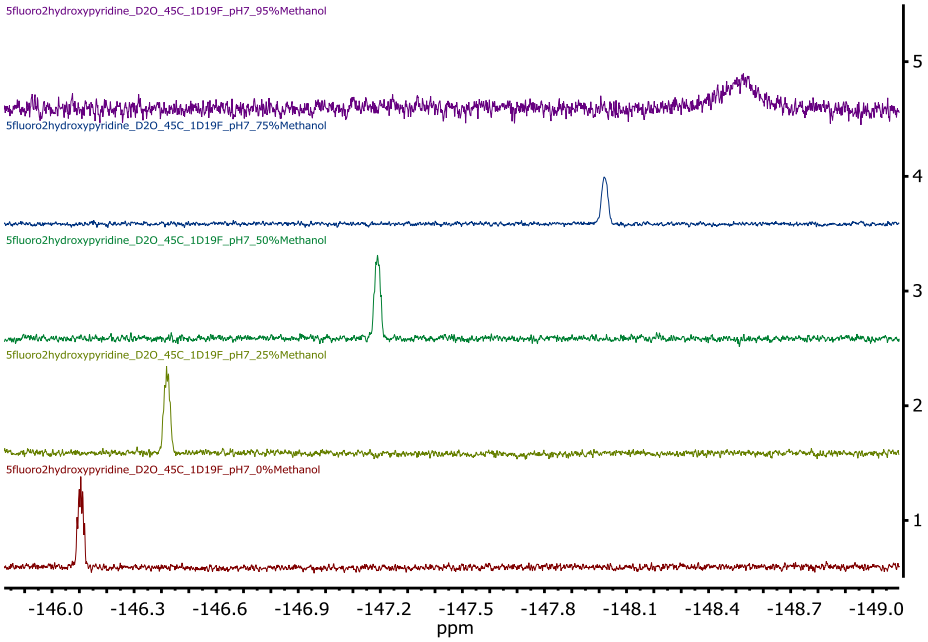

Appendix 32 1D 19F spectra of 5-MFHP with decreasing polarity (0-95% Water:Methanol) at 45°C.

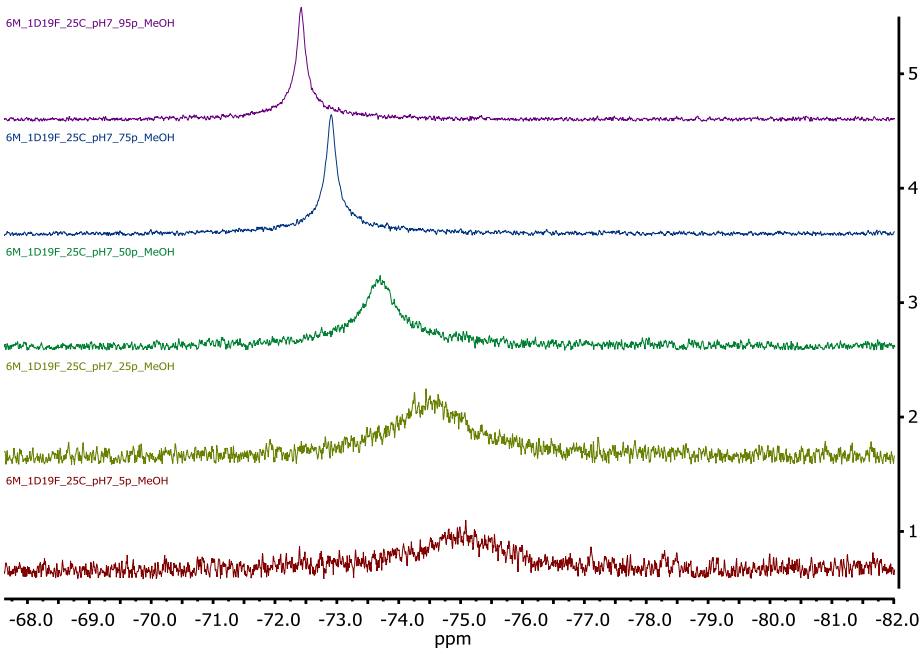

Appendix 33 1D 19F spectra of 6-MFHP with decreasing polarity (0-95% Water:Methanol) at 25ºC.

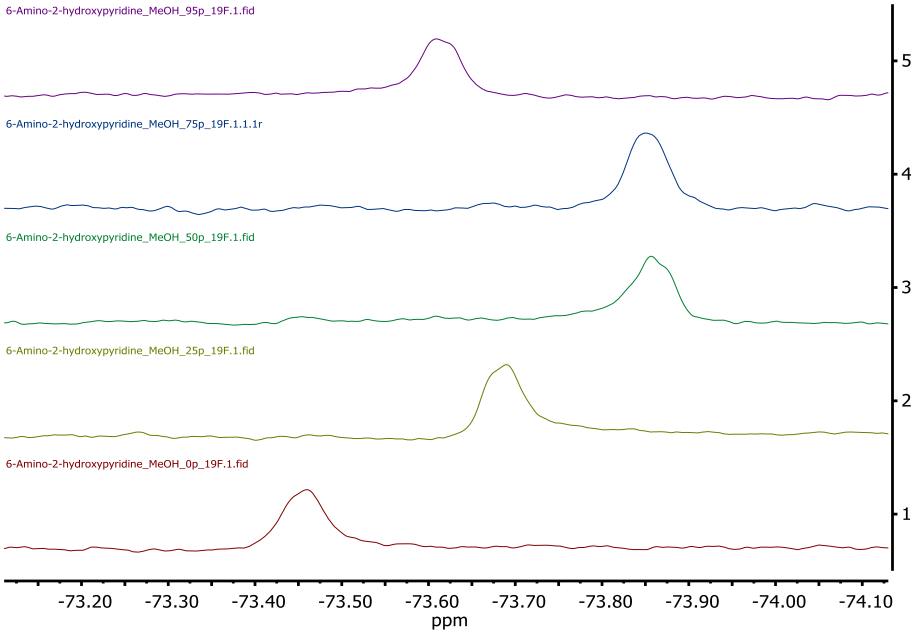

Appendix 34 1D ^{19}F spectra of 6-MFAP with decreasing polarity (0-95% Water:Methanol) at 25ºC.

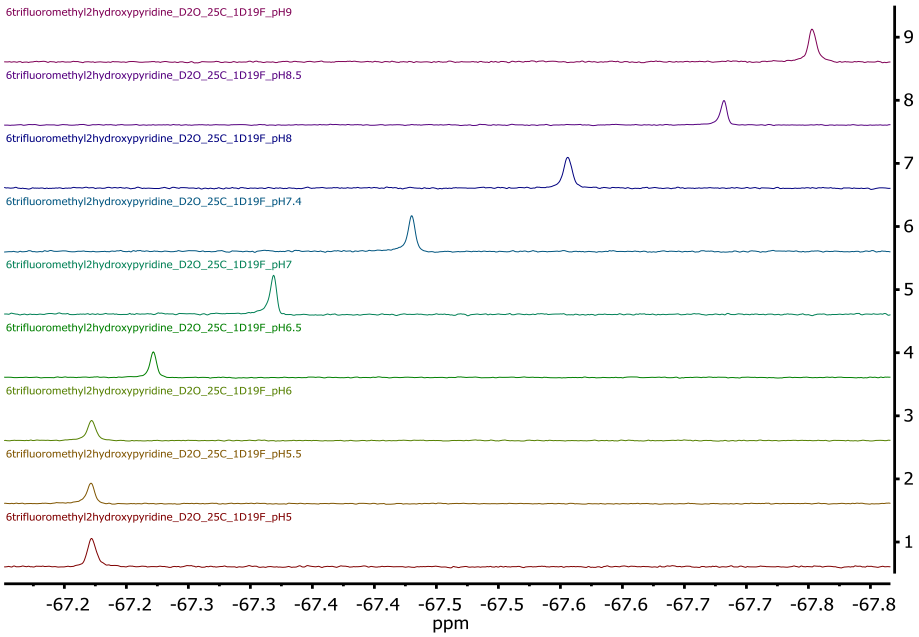

Appendix 35 1D ^{19}F spectra of 6-TFHP with increasing pH (pH 5-9) at 25ºC.

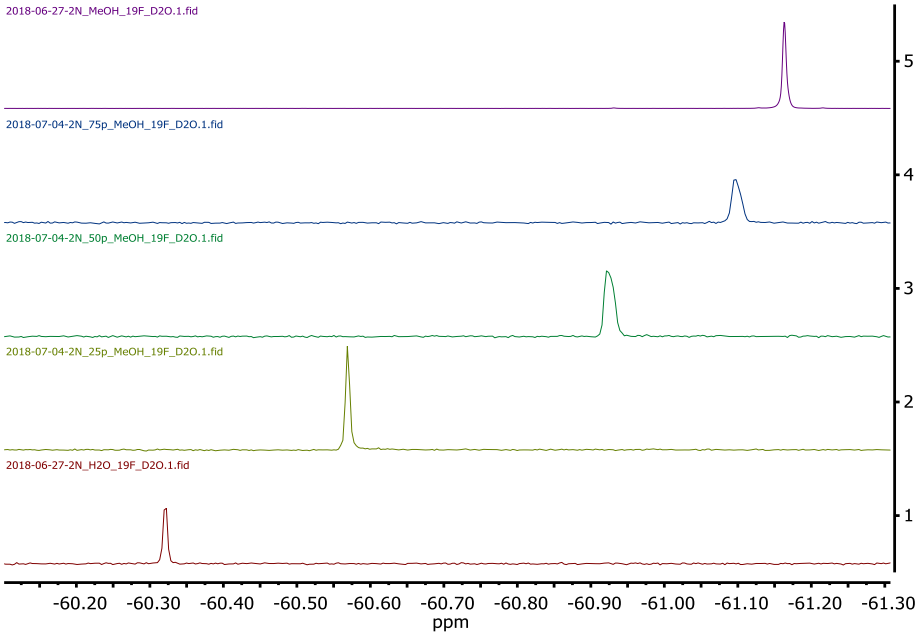

Appendix 36 1D ^{19}F spectra of 5-amino-2-nitrobenzotrifluoride with decreasing polarity (0-100% Water:Methanol) at 25ºC.

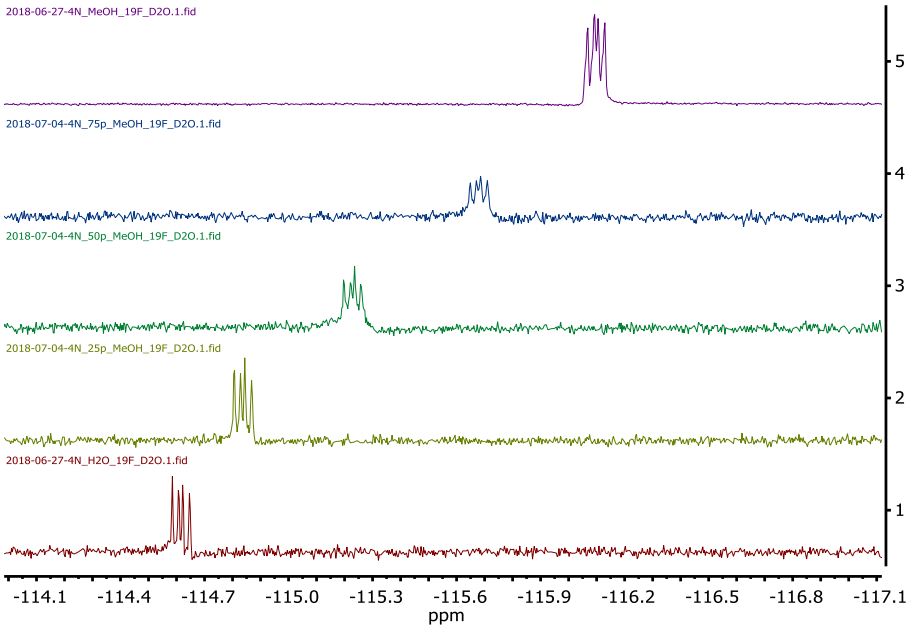

Appendix 37 1D ^{19}F spectra of 3-fluoro-4-nitroaniline with decreasing polarity (0-100% Water:Methanol) at 25ºC.

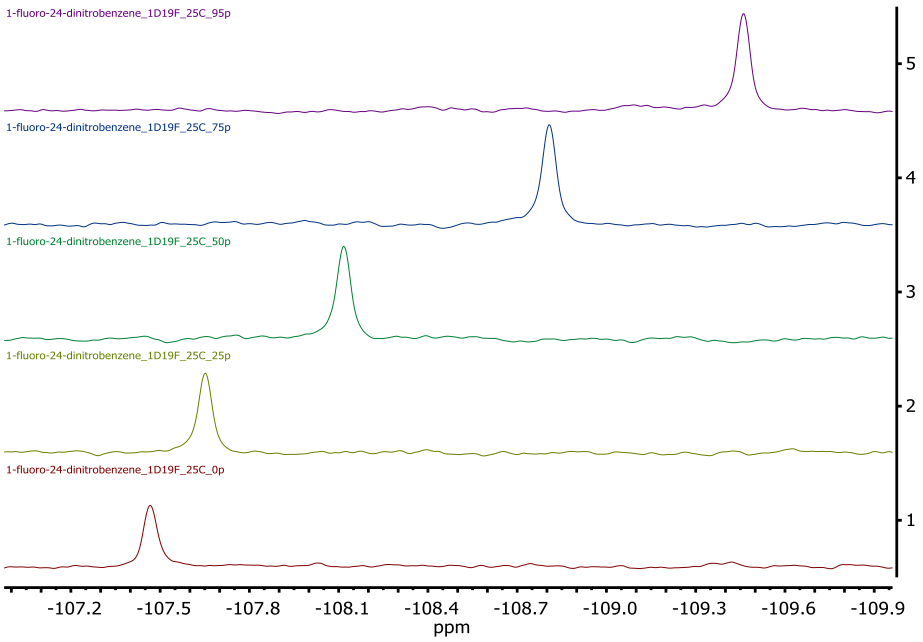

Appendix 38 1D ^{19}F spectra of 1-fluoro-2,4-dinitrobenzene with decreasing polarity (0-95% Water:Methanol) at 25ºC.

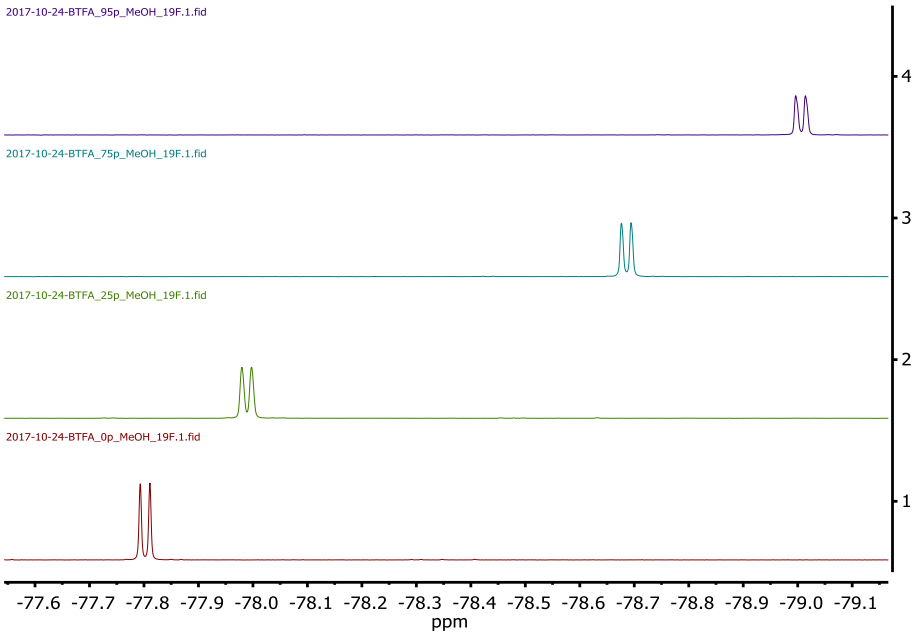

Appendix 39 1D ^{19}F spectra of BTFP with decreasing polarity (0-95% Water:Methanol) at 25ºC.

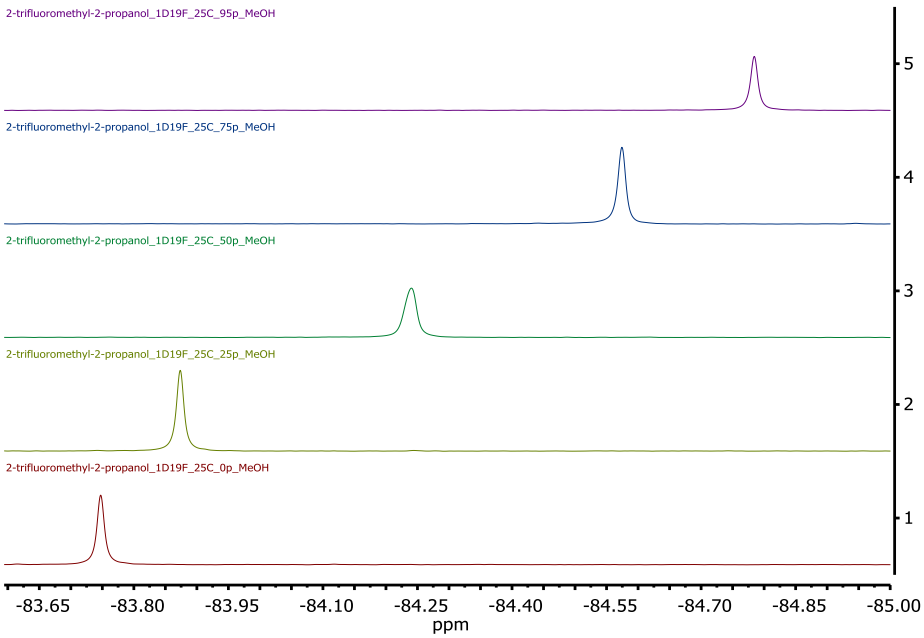

Appendix 40 1D ^{19}F spectra of 2-trifluoromethyl-2-propanol with decreasing polarity (5-100% Water:Methanol) at 25ºC.

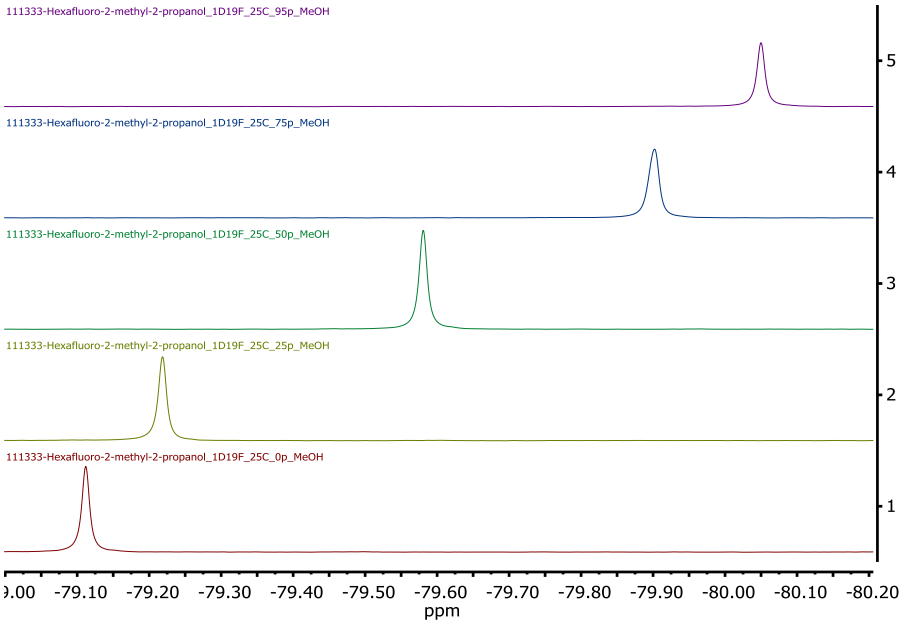

Appendix 41 1D ^{19}F spectra of 1,1,1,3,3,3-hexafluoro-2-methyl-2- propanol with decreasing polarity (0-95% Water:Methanol) at 25°C.

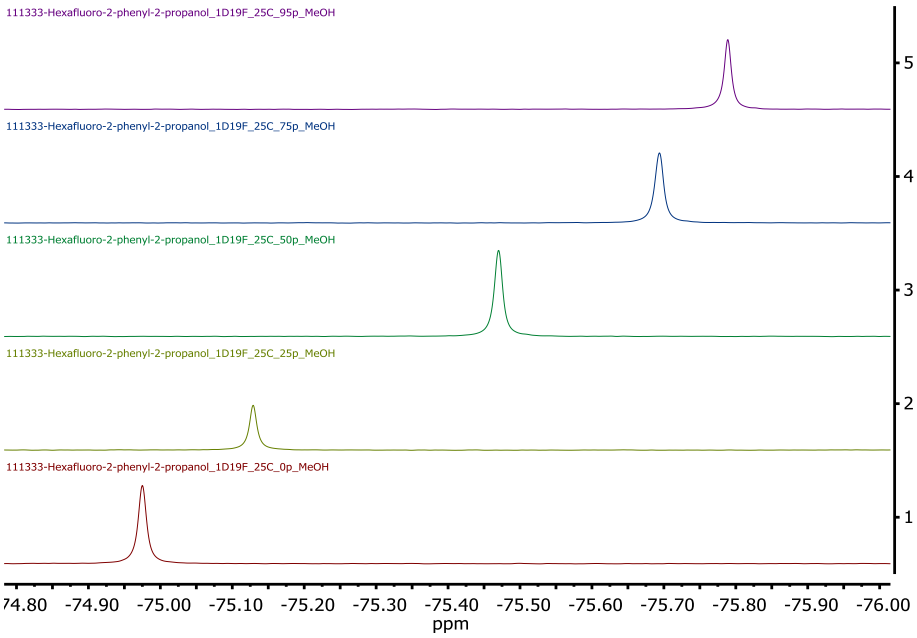

Appendix 42 1D ^{19}F spectra of 1,1,1,3,3,3-hexafluoro-2-phenyl-2- propanol with decreasing polarity (0-95% Water:Methanol) at 25°C.

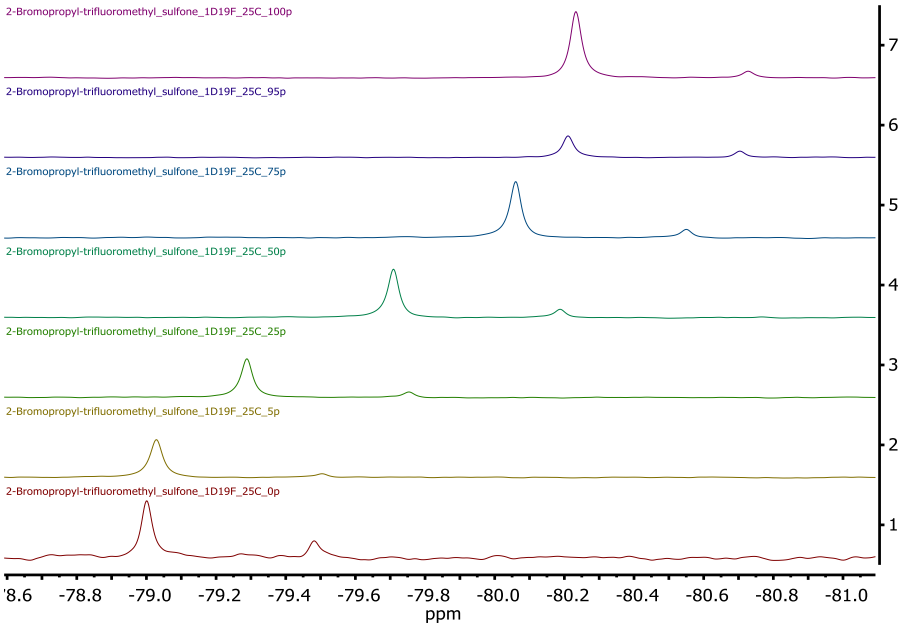

Appendix 43 1D ^{19}F spectra of BTFS with decreasing polarity (0-95% Water:Methanol) at 25ºC.

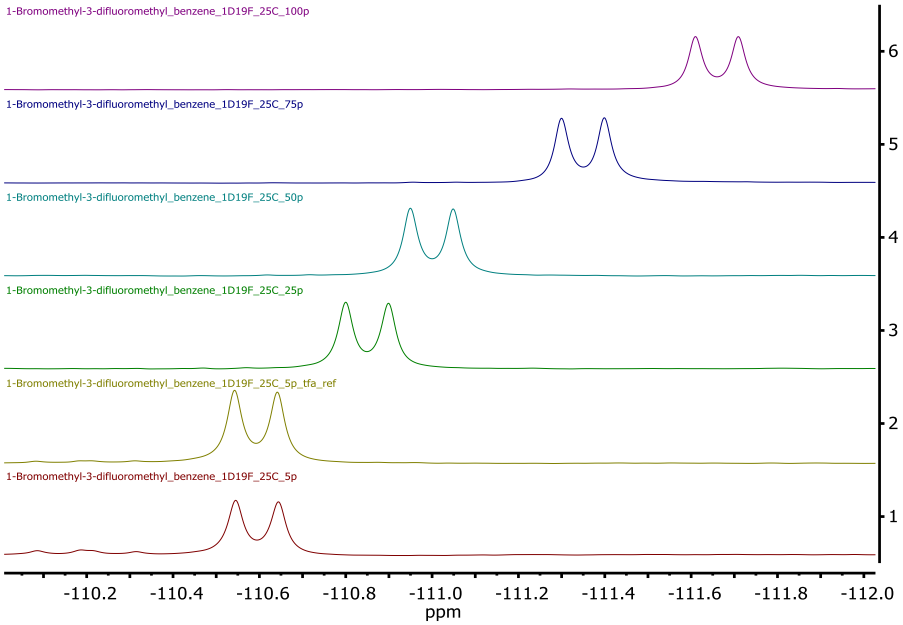

Appendix 44 1D ^{19}F spectra of 1-(bromomethyl)-3-(difluoromethyl) benzene with decreasing polarity (5-100% Water:Methanol) at 25ºC.

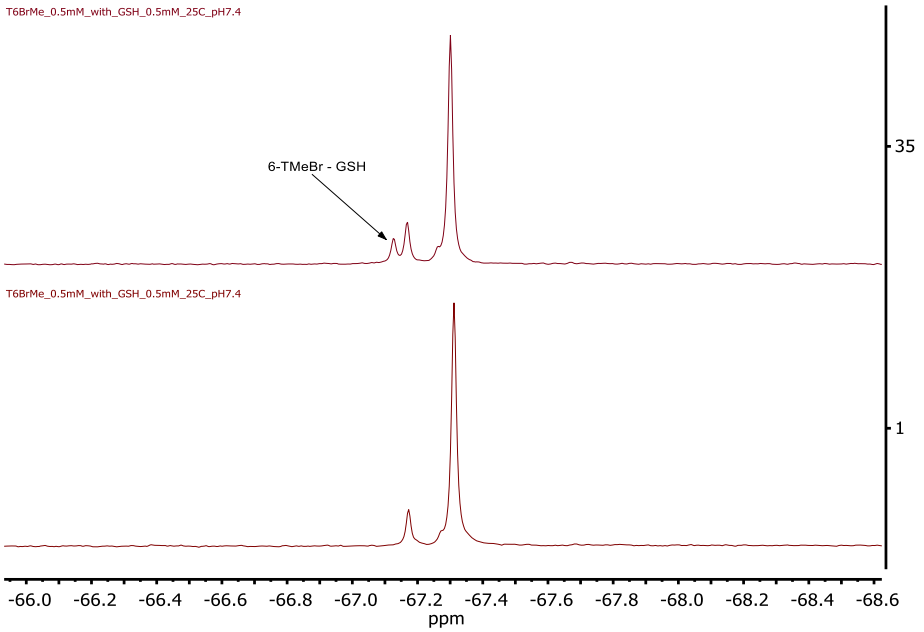

Appendix 45 Conjugation of 6-TMeBr to the cysteine on GSH at 25C and pH 7.4. Reaction was left overnight and monitored using ^{19}F NMR.

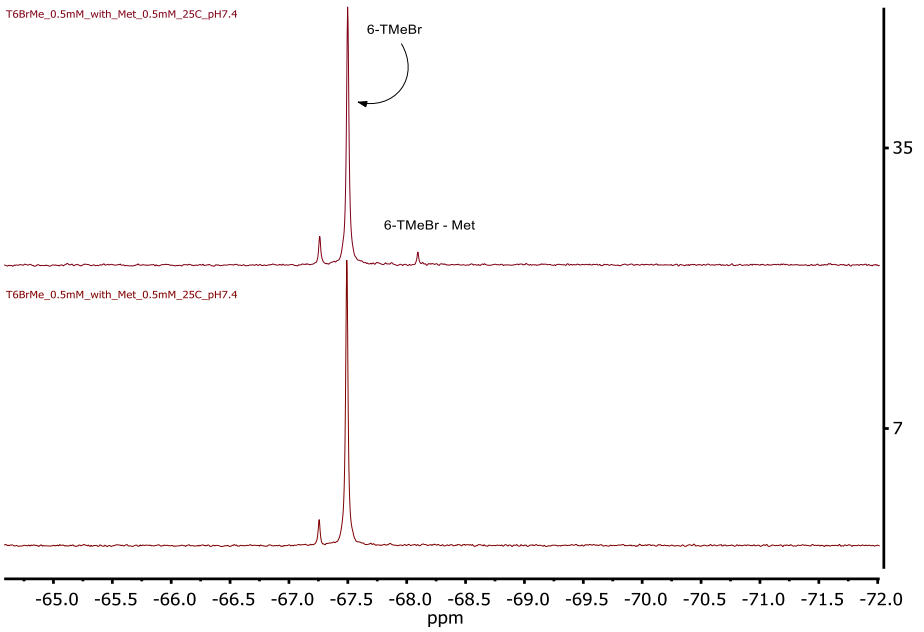

Appendix 46 Conjugation of 6-TMeBr to methionine at 25C and pH 7.4. Reaction was left overnight and monitored using ^{19}F NMR.

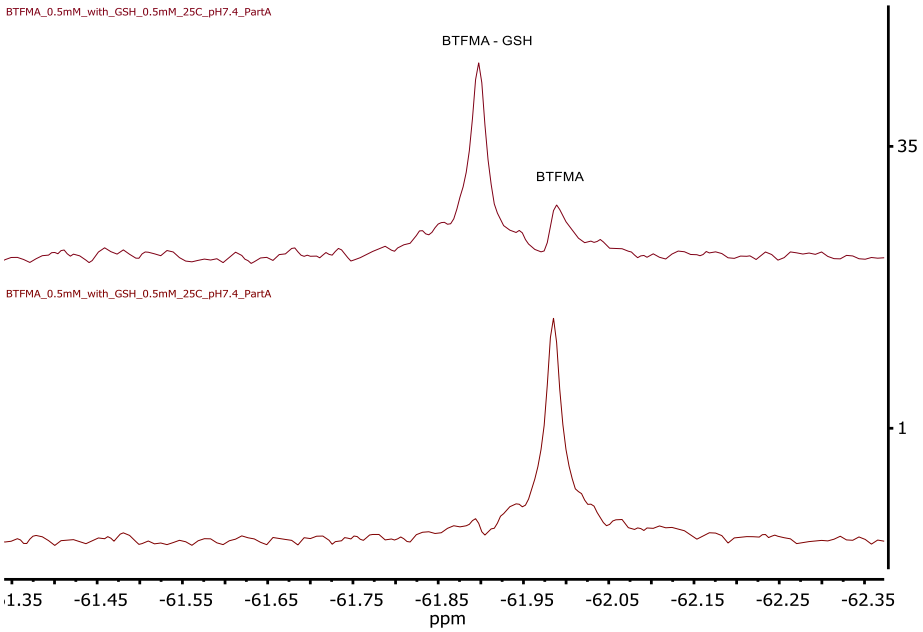

Appendix 47 Conjugation of BTFMA to the cysteine on GSH at 25C and pH 7.4. Reaction was left overnight and monitored using ^{19}F NMR.

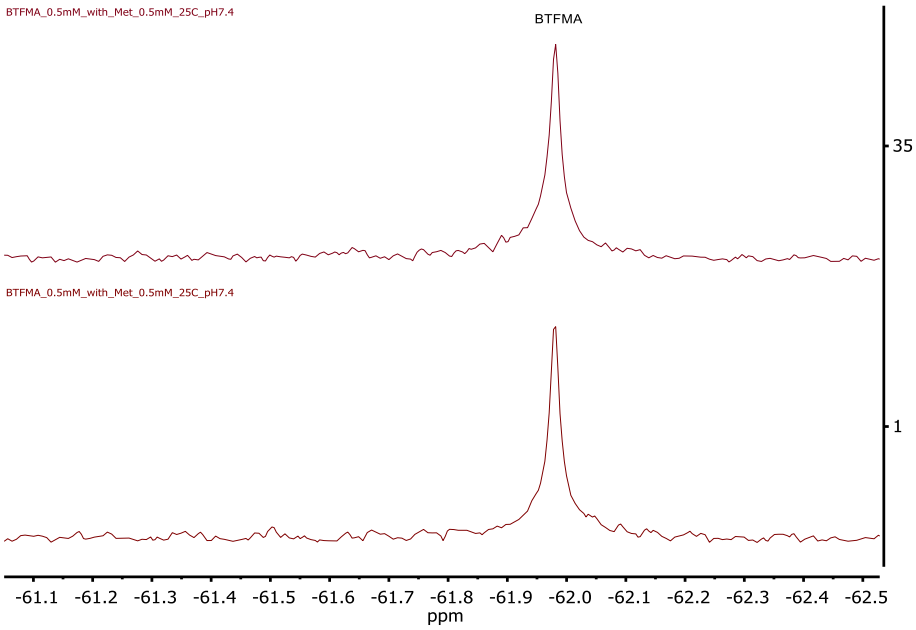

Appendix 48 Conjugation of BTFMA to methionine at 25C and pH 7.4. Reaction was left overnight and monitored using ^{19}F NMR.

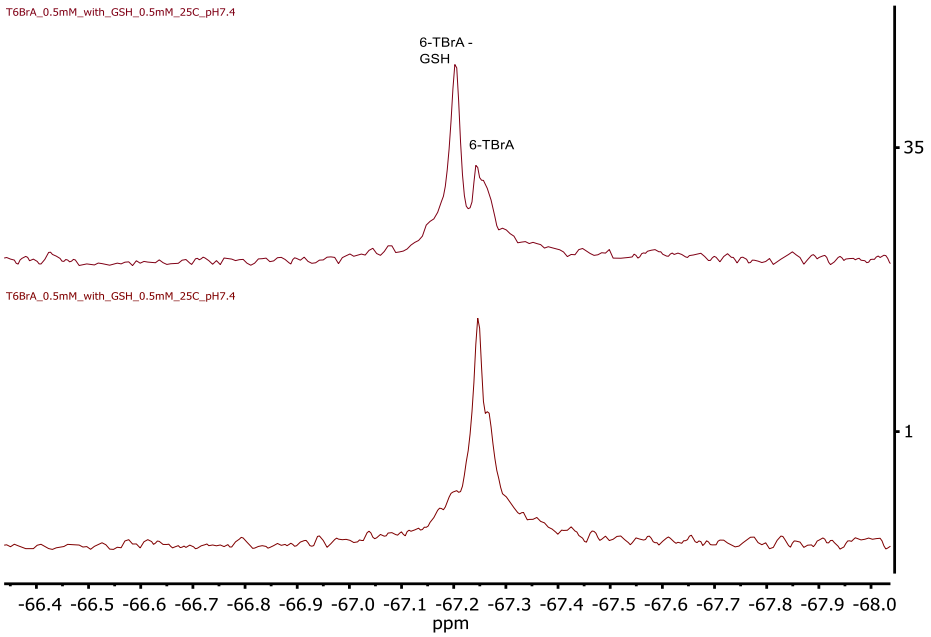

Appendix 49 Conjugation of 6-TBrA to the cysteine on GSH at 25C and pH 7.4. Reaction was left overnight and monitored using ^{19}F NMR.

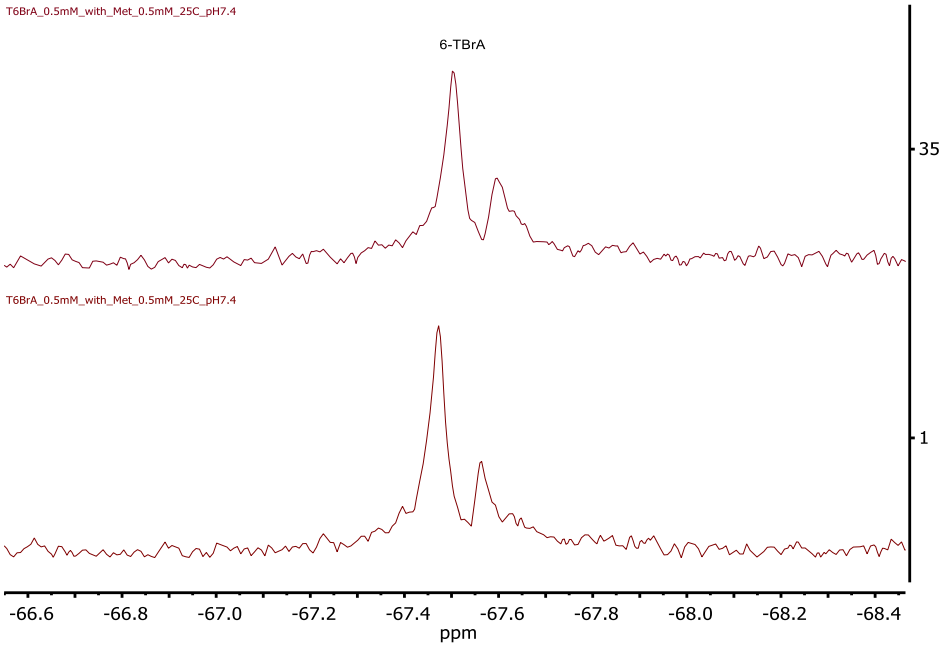

Appendix 50 Conjugation of 6-TBrA to methionine at 25C and pH 7.4. Reaction was left overnight and monitored using ^{19}F NMR.

Copyright Acknowledgements